

HEAT TRANSFER FROM FINNED TUBES UNDER  
MODERATE SCALING CONDITIONS

by

HENRY KARL MCCLUER

A THESIS

submitted to

OREGON STATE COLLEGE

in partial fulfillment of  
the requirements for the  
degree of

MASTER OF SCIENCE

June 1957

APPROVED:

Redacted for Privacy

---

Associate Professor of Chemical Engineering

In Charge of Major

Redacted for Privacy

---

Head of the Chemical Engineering Department

Redacted for Privacy

---

Chairman of School Graduate Committee

Redacted for Privacy

---

Dean of Graduate School

Presented June, 1957

Typed by Candis Travis Letter Shop

## ACKNOWLEDGMENT

The author wishes to thank Dr. J. G. Knudsen for the many hours he spent helping with this investigation. He also wishes to thank the Wolverine Tube division of the Calumet and Hecla Consolidated Copper Corporation for supplying the tubes used in this investigation and the Engineering Experimental Station of Oregon State College for sponsoring this investigation through a Research Assistantship.

## TABLE OF CONTENTS

	Page
INTRODUCTION - - - - -	1
LITERATURE AND THEORY	
The Mechanism of Scale Formation - - - - -	4
The Determination of Individual Heat Transfer Coefficients by Wilson's Method	7
Heat Transfer Coefficients on Finned Tubes in Annuli - - - - -	9
EXPERIMENTAL	
Apparatus - - - - -	12
The Experimental Heat Exchanger - - - - -	12
The Entrance and Exit Calming Sections - - -	13
The Tubes Tested in the Heat Exchanger - - -	19
The Cold Stream System - - - - -	22
The Hot Stream System - - - - -	25
Temperature Measurement - - - - -	26
Flow Measurement - - - - -	27
PROCEDURE - - - - -	29
DISCUSSION	
Scale Formation on the Finned Tubes - - - - -	32
Correlation of the Finside Heat Transfer Coefficients - - - - -	46
Comparison of the Experimental Scaling Factors to those Recommended by the Tubular Exchanger Manufacturers Association - - - - -	53
RECOMMENDATIONS - - - - -	56

TABLE OF CONTENTS (CONT.)

	Page
CONCLUSIONS - - - - -	58
BIBLIOGRAPHY - - - - -	59
APPENDIX	
Experimental Data - - - - -	60
Sample Calculations - - - - -	72

## TABLE OF ILLUSTRATIONS

		Page
Figure 1	Photograph of the experimental apparatus - - - - -	14
Figure 2	Schematic flow diagram of the experimental system - - - - -	15
Figure 3	Cross-section of the experimental annulus - - - - -	17
Figure 4	Cross-section of a calming section- -	18
Figure 5	Photograph of a calming section - - -	20
Figure 6	Scaling plot for the 5 fin/inch tube-	34
Figure 7	Scaling plot for the 7 fin/inch tube-	35
Figure 8	Scaling plot for the 9 fin/inch tube-	36
Figure 9	Scaling plot for the 19 fin/inch tube	37
Figure 10	Sketch of flow patterns developed between the fins - - - - -	40
Figure 11	Effective finside film coefficient vs. annular fluid Reynolds number - -	47
Figure 12	Effective Nusselt number substituted into equation (4) - - - - -	48
Figure 13	Apparent finside film coefficient vs. annular fluid Reynolds number - -	51
Figure 14	Apparent Nusselt number substituted into equation (4) - - - - -	52
Figure 15	Comparison of experimental and TEMA recommended fouling factors - - - - -	55
Figure 16	Solubility of calcium sulphate in water vs. temperature - - - - -	60
Figure 17	Wilson plot for the 5 fin/inch tube -	61

## TABLE OF ILLUSTRATIONS (CONT.)

	Page
Figure 18 Wilson plot for the 7 fin/inch tube -	62
Figure 19 Wilson plot for the 9 fin/inch tube -	63
Figure 20 Wilson plot for the 11 fin/inch tube-	64
Figure 21 Wilson plot for the 19 fin/inch tube-	65
Figure 22 Centigrade thermometer calibrations -	66
Figure 23 Centigrade thermometer calibrations -	67
Figure 24 Fahrenheit thermometer calibrations -	68
Figure 25 Fahrenheit thermometer calibrations -	69
Figure 26 Cold stream manometer calibration - -	70
Figure 27 Hot stream manometer calibration - -	71

## NOMENCLATURE

A	area - sqft
b	empirical constant
C	empirical constant - hr-sqft- $^{\circ}$ F/BTU
$C_p$	heat capacity - BTU/lb- $^{\circ}$ F
D	diameter - feet
f	fouling factor - dimensionless
h	individual heat transfer coefficient - BTU/hr-sqft- $^{\circ}$ F
k	thermal conductivity - BTU-ft/hr-sqft- $^{\circ}$ F
n	empirical constant - dimensionless
Nu	Nusselt number - dimensionless
Pr	Prandlt number - dimensionless
Q	heat transfer rate - BTU/hr
R	resistance to heat transfer - hr-sqft- $^{\circ}$ F/BTU
Re	Reynolds number - dimensionless
S	fin spacing - feet
t	temperature difference - $^{\circ}$ F
$U_o$	overall heat transfer coefficient - BTU/hr-sqft- $^{\circ}$ F
V	velocity - ft/sec
W	fin height - feet
	viscosity - lb/ft-sec
	weight density - lb/cuft
$\phi$	Gardner fin efficiency - dimensionless



## NOMENCLATURE (CON'T)

Subscripts

app apparent

e equivalent

eff effective

f fin

is inside

o overall

os outside

p prime

s scale

w wall

# HEAT TRANSFER FROM FINNED TUBES UNDER MODERATE SCALING CONDITIONS

## INTRODUCTION

The deposition of scale on heating surfaces and the subsequent reduction of the heat transfer rate is a major problem in industrial heat transfer operations. Chemical additives which substantially reduce scale formation may be employed in steam boiler operation where the condensate is collected and returned to the boiler feed water supply and in other instances where the treated water is recycled. However, most heat transfer operations require a large amount of cooling water which is not recycled but is released after only one pass through a heat exchanger. In this situation, chemical treatment of the water to reduce scale formation is not economical. These heat exchangers must be operated while in the scaled condition.

If heat transfer equipment is to operate in the scaled condition, it must be designed with sufficient capacity to provide the required heat transfer rates through the scale deposits. The effect of these deposits on the heat transfer rate is taken into account by including a "fouling factor" in the summation of heat transfer resistances which is used in the design calculations.

The Tubular Exchanger Manufacturers Association has published a list of recommended fouling factors to be used

in the design of plain tube exchangers for various operating conditions (8, pp.47-51). These fouling factors have been compiled from a large number of industrial cases and are widely used in heat exchanger design. However, very little information on the behavior of finned tubes under scaling conditions has been reported. Therefore, designers of finned tube heat transfer equipment have used the plain tube fouling factors. The purpose of this investigation was to obtain information concerning scale formation on transverse finned tubes and to compare finned tube fouling factors with those recommended by the Tubular Exchanger Manufacturers Association for plain tubes.

A study of the literature on scale formation shows that there are three basic types of scale:

- 1 - that deposited from water containing calcium and related minerals which is called "water hardness,"
- 2 - that formed by corrosion and galvanic reaction of the metals in heat transfer equipment,
- 3 - that of an organic nature which either grows in the cooling water or is deposited from organic fluids used as heat exchange media.

The present investigation studied the scaling characteristics of hard water scales on transverse finned tubes.

Since calcium sulphate is one of the major constituents of most hard water scales, scale formed from this salt was used in this study.

The investigation involved the experimental determination of overall heat transfer coefficients in a double

pipe heat exchanger containing a transverse finned tube. The cold annular fluid was a saturated solution of calcium sulphate in water, and the hot inner fluid was heated water under pressure. The effect of the scale deposited on the tube was indicated by the change of the overall heat transfer coefficient with time. By means of the method of Wilson (9, pp.47-82), the individual film heat transfer coefficients were determined, and the fouling factors of the scale deposits were calculated using these coefficients.

In addition, the film coefficients measured on the finned side of the tubes were compared with an equation developed by Knudsen and Katz (4, pp.490-500). This equation relates the finned side film coefficient on a transverse finned tube in an annulus to the annular dimensions and to the velocity and physical properties of the annular fluid.

## LITERATURE AND THEORY

### The Mechanism of Scale Formation

There has been extensive investigation of the formation of hard water scale on boiler heat transfer tubes; and many individual cases of hard water scaling on plain and finned tubes in industrial operation have been reported. However, no controlled, analytical studies of hard water scale formation on transverse finned tubes have been found in the literature.

The cases of hard water scaling on finned tubes in industrial operation which have been reported are individual and dependent on the local situation so that they yield little information to a controlled study of general finned tube scaling.

The studies of hard water scaling on plain boiler tubes were done using considerably higher temperatures and heat transfer rates than those used for this investigation and are therefore not directly applicable to this study. However, a study of boiler tube scaling by Partridge (6, pp.67-84) presents an excellent theory for the plain tube scaling mechanism which can be modified to fit the finned tube situation.

Partridge observed that the deposition of scale on boiler heating surfaces and the subsequent increase in

scale thickness is primarily caused by salts which are slightly soluble in water and which have an inverse solubility curve in the range of temperatures used in steam boiler operations. He determined that the initial deposition of scale crystals occurs from a supersaturated solution of the salt through one of two mechanisms. One, since the majority of the scale forming salts decrease in solubility with increasing temperature, the stagnant film of water adjacent to a heat transfer surface tends to be supersaturated with the salt even though the bulk of the solution may be below the saturation point. This supersaturation within the stagnant film can be relieved by spontaneous crystallization promoted by the minute irregularities in the heat transfer surface. Or, two, if the heat transfer rate is great enough to cause bubbles to be evolved from the heat transfer surface, the solute from the vaporized solution is directly deposited in rings of minute crystals at the solid-liquid-vapor interface formed at the outer ring of the bubble.

Investigations by Partridge indicate that the latter mechanism undoubtedly accounts for the deposition of almost all the initial scale nuclei on heat transfer surfaces from which vaporization of hard water is taking place. However, after the scale layer becomes thick enough to reduce the heat transfer rate to a point where

bubbles are no longer formed, the scale layer increases in depth through the first mechanism.

The present investigation of hard water scale deposition was carried out at temperatures which were always below the bubble point of the calcium sulphate solution flowing in the annulus. Therefore, the scale was formed by crystallization from the supersaturated film layer adjacent to the heat transfer surface.

It is probable that the behavior of plain tubes under scaling conditions is quite different from that of transverse finned tubes since turbulence is created near the surface of the tube by the fins. During their investigation of heat transfer and pressure drop in annuli, Knudsen and Katz (4, pp.490-500) studied the flow patterns of water flowing in the annular space of a double pipe heat exchanger containing an inner transverse finned tube. Photographs of the water flow patterns show that one or more eddies are formed between the fins when there is turbulent flow in the annulus. (Figure 10) The study indicates that the ratio of fin height to fin spacing,  $W/S$ , (Figure 3) may be used to predict the flow patterns which will develop between the fins.

The presence of the eddies between the fins will effect the laminar sublayer adjacent to the heat transfer surface from which the scale is crystallizing. The more

completely the eddy or eddies fill this space, the thinner the laminar sublayer will be. Therefore, it may be proposed that the ratio of fin height to fin spacing will effect the amount of scale which will be deposited between the fins.

This proposal is developed further in the discussion section where the scaling data from this study is presented.

#### The Determination of Individual Heat Transfer Coefficients by Wilson's Method

In 1915, Wilson (9, pp.47-82) introduced a graphical method which may be used to separate the overall resistance to heat flow through a heat transfer tube, ( $R_o$ ), into its four major components: the film resistance on the inner surface of the tube, ( $R_{is}$ ), the resistance of the tube wall, ( $R_w$ ), the resistance of any scale deposit on the tube, ( $R_s$ ), and the film resistance on the outer surface of the tube, ( $R_{os}$ ). The overall heat transfer coefficient is composed of the several heat transfer resistances as follows:

$$1/U_o = R_o = R_{is} + R_w + R_s + R_{os} \quad (1)$$

where  $U_o$  is the overall heat transfer coefficient and  $R_o$  is the overall resistance to heat transfer.

The film resistance to heat transfer between a fluid and a tube wall is related to the physical properties and velocity of the fluid as follows:

$$hD/k = 0.023(DV\rho/\mu)^{0.8}(C_p\mu/k)^{0.4} \quad (2)$$



where the heat transfer coefficient "h" is the reciprocal of the film resistance. The resistance of the tube wall and of the scale deposit are essentially constant although their thermal conductivities vary somewhat with temperature. Therefore, if the temperatures of the fluids on both sides of the heat transfer surface are held constant, the physical properties of both fluids remain constant; and the overall resistance to heat transfer is proportional to the velocities of the two fluids.

During this investigation, the temperatures of both fluid streams and the velocity of the fluid flowing within the transverse finned tubes were held constant. Hence,  $R_{is}$ ,  $R_w$ , and  $R_s$  remained constant, and equation (1) may be rewritten as:

$$1/U_o = C + R_{os} = C + 1/b(V)^n \quad (3)$$

where b is an empirical constant which describes the physical properties of the fluid in the annulus and where

C is  $R_{is} + R_w + R_s$ .

For plain tubes, the reported value of n is 0.8. For transverse finned tubes, Knudsen and Katz reported the value of n is 0.87. In the present study, it was found that n had a value of 0.87.

Equation (3) indicates that a plot of  $1/U_o$  versus  $1/(V)^n$  is a straight line having an intercept of C and a

slope of  $1/b$ . This plot is a Wilson plot. Such plots were made for all five of the transverse finned tubes used for this investigation while they were clean and scale free (Figures 17, 18, 19, 20 and 21). During the scaling runs, the same inner fluid velocity and fluid temperatures as those used for the Wilson plots were maintained. Thus, any increase in the value of  $C$  during the scaling runs was caused by the added resistance of the scale deposit.

#### Heat Transfer Coefficients on Finned Tubes in Annuli

Knudsen and Katz (4, pp.490-500) developed an equation of the Dittus-Boelter form for predicting the effective fin side heat transfer coefficient from transverse finned tubes to fluids in turbulent flow within an annulus. Their correlation employs the usual Nusselt, Prandlt, and Reynolds numbers and also utilizes two dimensionless groups which describe the geometry of the annulus. The fin height, ( $W$ ), the fin spacing, ( $S$ ), and the equivalent diameter of the annulus, ( $D_e$ ), are the annular dimensions used in these two additional groups (Figure 3).

The equation of Knudsen and Katz is

$$Nu_{eff} = (0.039)(Re)^{0.87}(Pr)^{0.4}(S/D_e)^{0.4}(W/D_e)^{-0.19} \quad (4)$$

where  $Nu_{eff}$  is the Nusselt number determined using an effective area for the finned side of the transverse

finned tube and  $Re$  is the Reynolds number determined using the equivalent diameter of the annulus.

The effective area of the finned surface of a transverse finned tube must be used instead of the total area because of the temperature gradient along the length of the fins. Consider the general equation for heat transfer from a surface:

$$Q = hA \Delta t \quad (5)$$

It is apparent that the heat transfer rate is directly proportional to the total area and to the temperature difference for a constant film heat transfer coefficient. The fins which are attached to the surface on a finned tube greatly increase the total heat transfer area; and it would be expected that the rate of heat transfer would be proportionally increased. However, since the fin temperature decreases towards the tip of the fin, the effectiveness of the finned area is reduced.

To account for this decrease in temperature difference towards the tip of the fins, Gardner developed an efficiency factor for the finned area (1, pp.621-631). This factor reduces the total finned area to an effective area transferring heat under the same temperature difference as the prime area at the base of the tube. The Gardner efficiency is defined as the ratio of the average temperature difference over the finned surface to that at

the base of the fins. Therefore, the total effective area is determined from:

$$A_{\text{eff}} = A_p + \phi A_f \quad (6)$$

where  $A_p$  is the prime area of the smooth tube without fins,  $\phi$  is the Gardner fin efficiency, and  $A_f$  is the area of the fins.

In the present investigation, the finned side film heat transfer coefficients were correlated in a manner similar to that used by Knudsen and Katz; and the correlation was compared to that of these authors. The results of the correlation and comparison are presented in the discussion section.

## EXPERIMENTAL

### Apparatus

The experimental apparatus consisted of a double pipe test heat exchanger and of accessory equipment which supplied cold fluid to the annulus and hot fluid to the inner tube of the exchanger. Flow rates were measured by means of calibrated orifices, and temperatures were determined by calibrated mercury thermometers. Figures 1 and 2 are a photograph and schematic flow diagram of the experimental apparatus. The calcium sulphate scale was deposited on the outer, finned surface of the inner tube of the annulus from the cold annular stream.

### The Experimental Heat Exchanger

Since it was desired to deposit a uniform scale over the finned surface of the inner tube of the annulus, it was necessary to minimize any flow disturbances due to entrance or exit effects within the exchanger. To do this, the annulus was made as long as practical, 71 diameters of the outer tube of the exchanger, and special entrance and exit calming sections were provided.

A smooth copper tube having an inside diameter of  $1.056 \pm 0.003$  inches constituted the outer tube of the test

heat exchanger, and a transverse finned tube constituted the inner tube of the annulus. The length of the exchanger was 8 feet, 10-1/2 inches exclusive of the end sections. The outer tube of the annulus was connected to the end sections by circular flanges made from 1/4 inch copper plate. These flanges were welded to the outer tube and were bolted to each end section with six 1/4-inch bolts on a 3-1/2 inch bolt circle. Gaskets and gasket compound were placed between the flanges and the end sections to assure a tight seal. The inner tubes used in the experimental heat exchanger are described below. Figure 3 shows a cross section of the experimental annulus.

#### The Entrance and Exit Calming Sections

Figure 4 is a detailed drawing of the identical entrance and exit sections of the exchanger. They are calming sections which were designed to produce a uniform flow throughout the exchanger. Four separate entrances to the calming sections were provided by the pipes, F, for an even distribution of the incoming annular fluid. The edges of the hole in flange A-1 were rounded, and the taper of the bushing, B, closely conformed to the fluid streamlines of the entering annular fluid. In this manner, exit and entrance effects were minimized. Since the inner tubes of

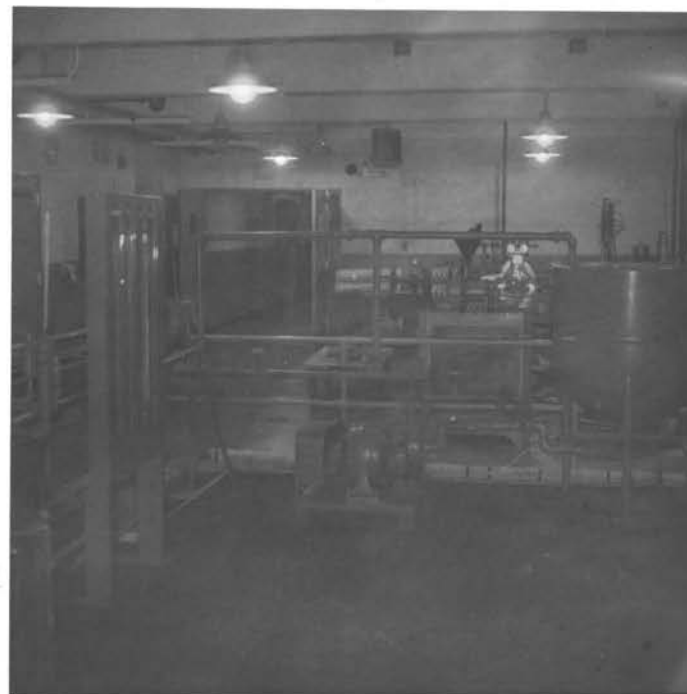


FIGURE 1  
PHOTOGRAPHS OF THE EXPERIMENTAL APPARATUS

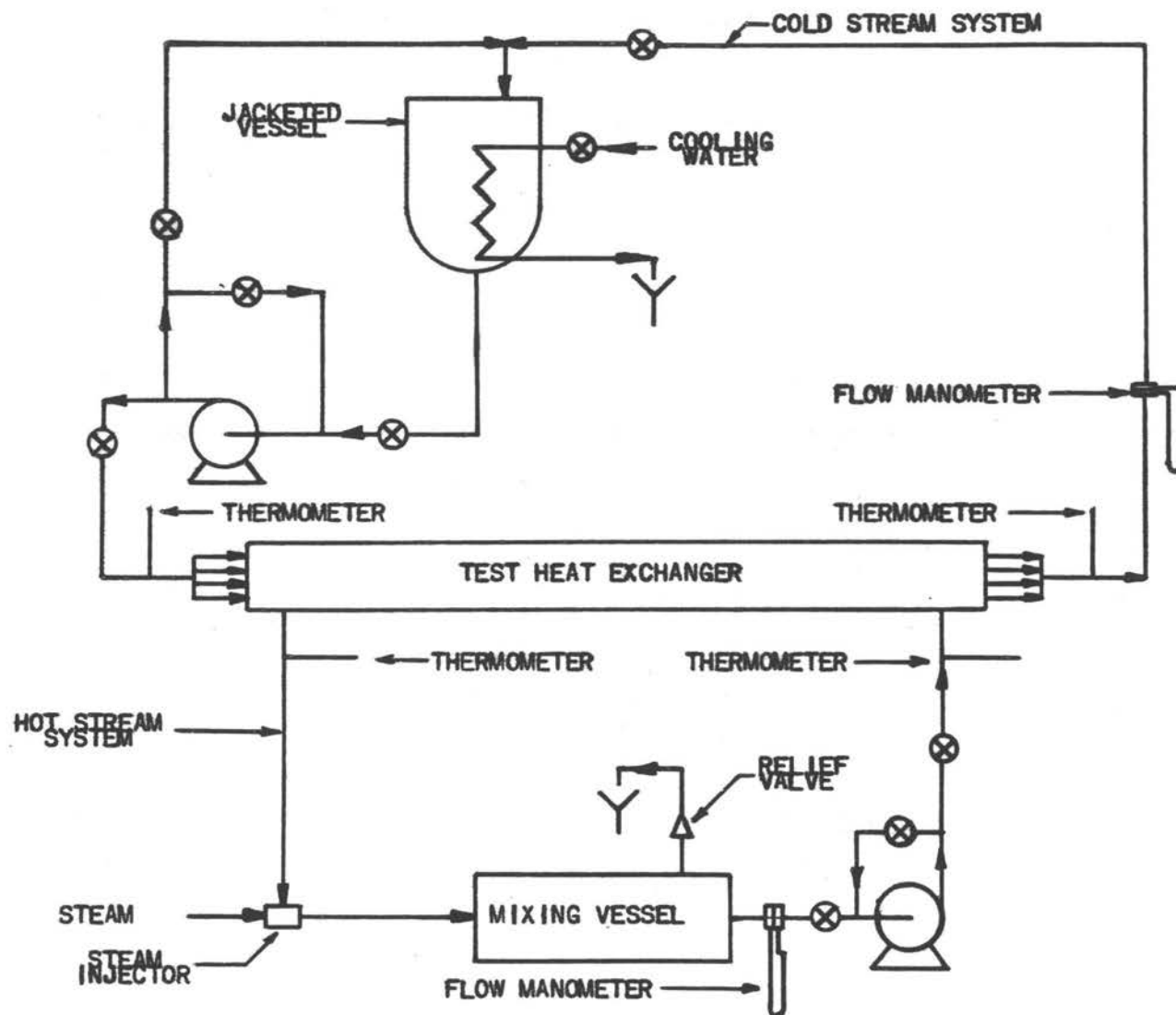


FIGURE 2 - SCHEMATIC FLOW DIAGRAM OF THE EXPERIMENTAL SYSTEM



the exchanger were frequently changed, it was necessary to provide packing glands in the two calming sections to facilitate the removal and replacement of these tubes.

Flanges A-1 and A-2 were machined from 3/4-inch boiler plate. The hole machined into the center of flange A-1 was the same diameter as the inside diameter of the outer tube of the annulus. The edges of the hole were rounded. Flange A-2 was made thicker at the center by welding on a circular piece of 3/4-inch boiler plate. Flange A-2 was machined to hold bushing, B, packing, C, floating ring, D, and packing gland, E. Four holes were drilled into flange A-2 on a 5-inch circle around the packing gland and were tapped with 3/4-inch standard pipe threads for the installation of the entrance pipes, F.

A 3-1/2 inch section of standard 6-inch steel pipe was placed between flanges A-1 and A-2 to form the calming sections. The flanges were bolted to either end of the 6-inch pipe with eight 5/16-inch bolts which were 5 inches long. Grooves were machined in both flanges to match ridges machined on the ends of the 6-inch pipe. Gaskets and gasket compound were employed to assure a leaktight joint. Figure 5 is a photograph of one of the assembled calming sections.

The bushing, B, was drilled through so that the hot

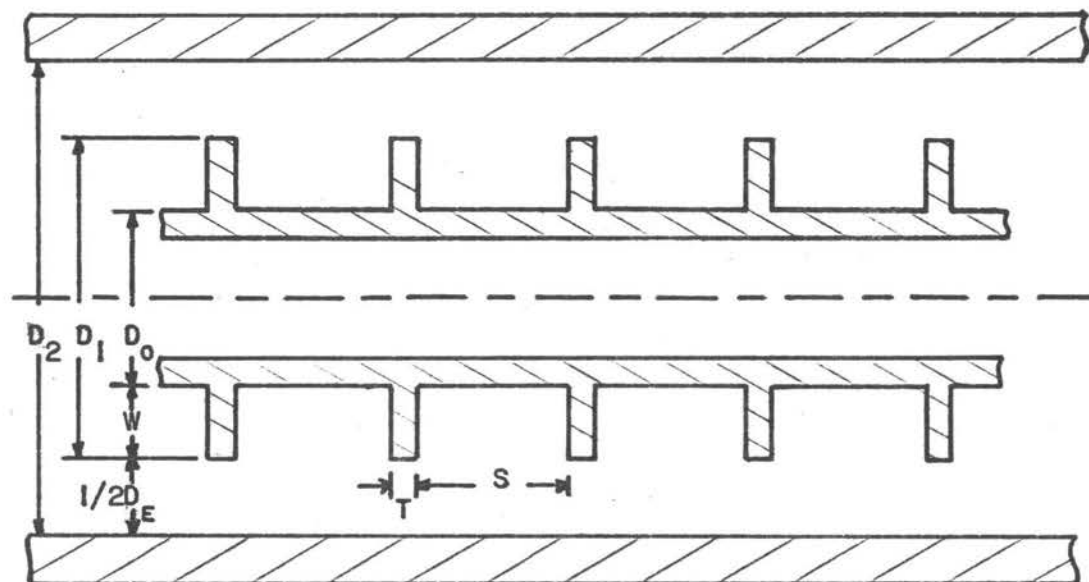


FIGURE 3 - CROSS-SECTION OF THE EXPERIMENTAL ANNULUS

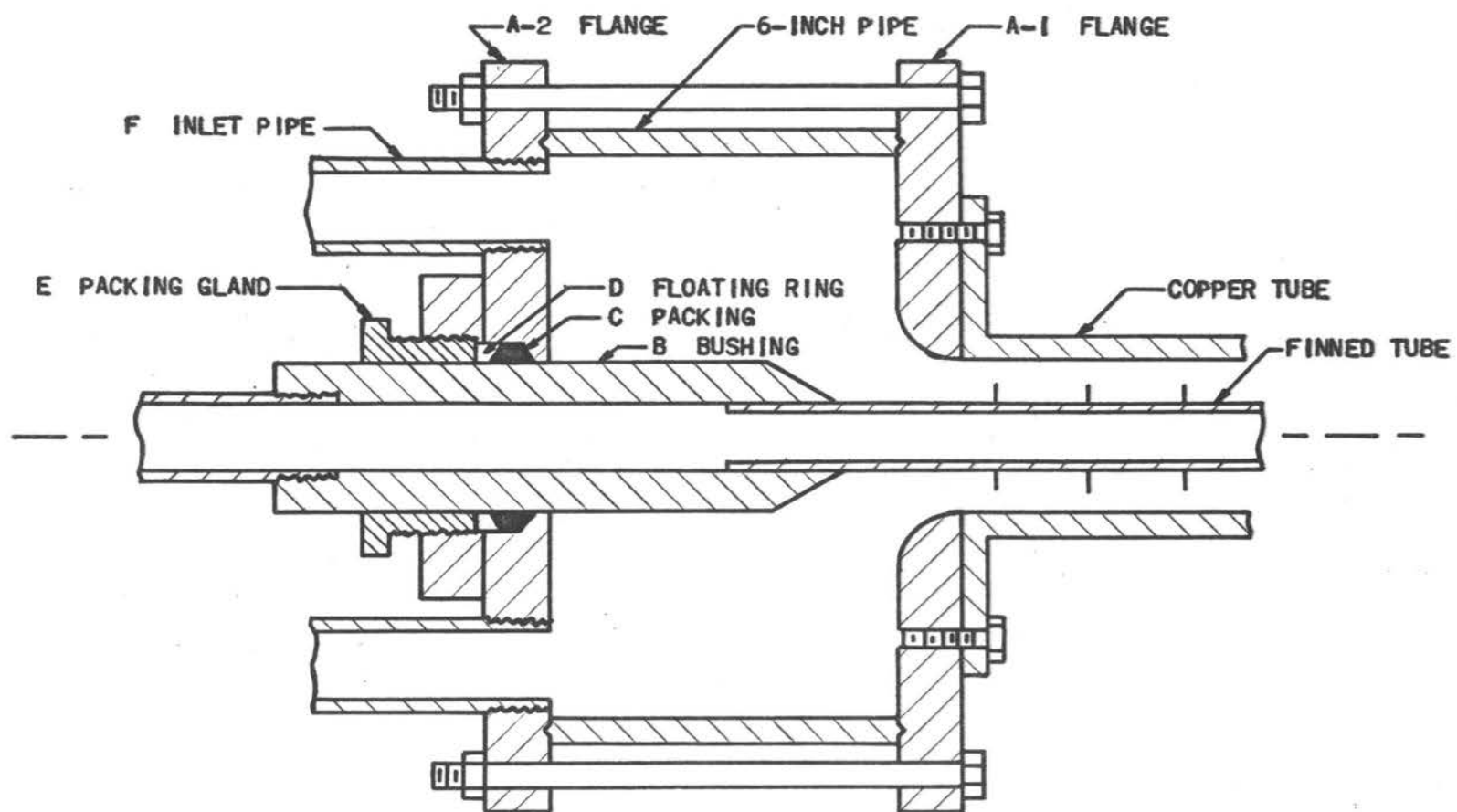


FIGURE 4 - CROSS-SECTION OF A CALMING SECTION

side fluid would pass through it into the inner tube of the annulus. The inner finned tube was soldered into the end of the bushing, and additional solder was added at the joint to prevent the hot stream fluid from leaking into the annular fluid. The outer end of the bushing was tapped with standard 3/4-inch pipe threads so the bushing could be easily connected to the hot stream piping. The taper on the end of the bushing, B, was approximately  $30^{\circ}$  to conform closely to the streamlines of the annular fluid entering the calming section through the pipes, F.

#### The Tubes Tested in the Heat Exchanger

Five different transverse finned tubes were tested during the investigation. These tubes had fin spacings of 5, 7, 9, 11, and 19 fins-per-inch. All of these tubes were manufactured and supplied through the courtesy of the Wolverine Tube Company, a division of the Calumet and Hecla Copper Company, Detroit, Michigan. The dimensions of these tubes are listed in Table I. For all calculations the fins were assumed to be of constant thickness from the base to the tip of the fin.

The finned tubes were soldered into the bushings, B, and were held in the annulus by the packing glands in the entrance and exit sections. Since the tubes were made of soft copper and were of considerable length, supports were

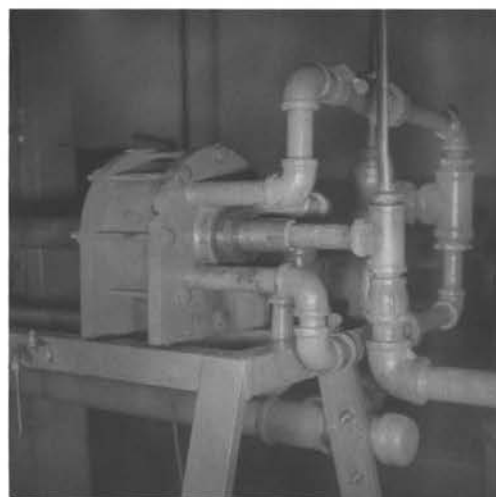


FIGURE 5

PHOTOGRAPHS OF A CALMING SECTION

TABLE I  
DIMENSIONS OF THE EXPERIMENTAL FINNED TUBES

Fins/inch (nominal)	5	7	9	11	19
Fins/inch (actual)	5.2	7.1	8.9	11.4	20.2
Diameter of fins - $D_f$ (inches)	0.996	0.889	0.874	0.768	0.863
Root diameter - $D_o$ (inches)	0.499	0.386	0.400	0.525	0.763
Fin height - $W$ (inches)	0.249	0.251	0.237	0.121	0.050
Fin thickness - $t$ (inches)	0.015	0.020	0.015	0.012	0.008
Fin spacing - $S$ (inches)	0.176	0.125	0.092	0.071	0.032
Finned length (feet)	7.833	7.833	7.833	8.042	8.167
Area of Primary - $A_p$ surface (sqft)	1.012	0.780	0.746	0.955	1.117
Area of extended - $A_f$ surface (sqft)	4.121	4.926	5.750	3.998	3.809
Total outside area (sqft)	5.133	5.707	6.496	4.953	4.926
Inside diameter - $D_i$ (inches)	0.303	0.242	0.244	0.494	0.745
$\frac{\text{Fin height}}{\text{Fin spacing}} = \frac{W}{S}$	1.414	2.008	2.576	1.704	1.562
Equivalent diameter ( $D_2 - D_f$ ) (inches)	0.060	0.167	0.182	0.288	0.193

required to keep the tubes centered in the annulus. These supports were made of 1/16-inch brass wire and were silver soldered to the fins. Three sets of supports were equally spaced along the length of the tube. Each set of supports consisted of three wire legs equally spaced around the circumference of the tube. Rothfus (7, p.2515) has shown that legs such as these have very little effect on the flow patterns in an annulus.

#### The Cold Stream System

The cold stream system supplied the artificially hardened water to the annulus of the experimental exchanger. This system consisted of a pump and motor, a jacketed saturation tank, two thermometers, and an orifice and manometer. Figure 1 is a schematic flow diagram showing the cold stream system.

The pump was a 2-inch by 1-1/2 inch centrifugal pump with a capacity of 40 gpm. It was driven by a 5 hp, 220 volt, 3-phase electric motor.

The cold water saturated with calcium sulphate flowed from the discharge of the pump into the entrance calming section of the experimental exchanger. Two by-passes on the pump were installed. One by-pass was used to control the flow rate of the hard water flowing into the annulus,

and the other was available to recycle part of the hard water stream back into the jacketed vessel for additional cooling.

From the exit calming section of the exchanger the hard water stream flowed through a metering orifice and into the jacketed vessel. The jacketed vessel had a double service in the system. It cooled the hard water before it was pumped back into the exchanger and resaturated the cooled water with calcium sulphate. Additional cooling surface was provided by three compact finned heat exchangers which were suspended in the upper portion of the vessel. The jacketed vessel had a round bottom which deflected the incoming stream of hard water so that enough turbulence was developed in the vessel to provide forced convection for the three exchangers. Lumps of pure calcium sulphate were placed in the jacketed vessel so that the cooled water pumped from the vessel into the experimental exchanger was saturated with the salt.

Since calcium sulphate has an inverse solubility in the temperature ranges used for this study (Fig. 16), the lumps were placed in the coolest portion of the system. This was at the bottom of the jacketed vessel. Thus, it was assured that the maximum amount of calcium sulphate would be dissolved in the cold stream. The calcium sulphate lumps



which were placed in the vessel had a diameter of approximately 2 inches. These large lumps were used to assure there would be no small particles of the salt circulating through the system which might clog up the piping or lodge between the fins on the tubes.

The calcium sulphate lumps were made from powdered plaster of Paris. The powder was mixed with water and molded into spheres of 4 to 6 inches diameter. After several days of drying, these spheres were broken into the 2-inch lumps. These lumps were dried for another week, and then they were placed in the jacketed vessel. Examination of the cold stream system after several weeks of operation showed that there was little disintegration of the lumps and that there were no particles of solid calcium sulphate circulating through the system.

All of the piping of the cold side system was 1-1/2 inch black iron pipe except for a short section of 2-inch black iron pipe leading from the bottom of the jacketed vessel to the suction side of the pump. Valves were placed in the system so that the flow rate to the experimental exchanger could be easily controlled and so that additional cooling of the hard water was possible through recycle back into the jacketed vessel.

### The Hot Stream System

The hot stream system of the experimental heat exchanger was made up of a pump and motor, a steam injector-heater, a small mixing vessel, two thermometers, and a metering orifice and manometer. Figure 1 is a schematic flow diagram showing the hot stream system. Hot water, rather than steam, was pumped through the inner tube of the annulus so that any irregularities in steam condensation and/or heat flux which might have developed would be eliminated.

The pump was a 1-inch by 3/4-inch centrifugal pump with a capacity of 10 gpm. It was driven by a 1/4 hp, 110 volt, 2-phase electric motor.

From the discharge side of the pump, the hot water flowed into the inner tube of the experimental heat exchanger. The cooled water from the exit of the exchanger then flowed into the steam injector-heater. This steam injector was a 1/2-inch by 3/4-inch Penberthy Silent Water Heater obtained from the Penberthy Injector Company of Detroit, Michigan. Steam at 65 psig from the laboratory supply was piped to the injector. The steam flow rate was controlled by a gate valve placed in the 1-inch line supplying steam to the system.

From the injector, the heated water flowed into a

small mixing vessel to assure complete condensation of the steam and a uniform temperature of the water leaving the vessel. This mixing vessel was made by welding steel flanges 6 inches square and 1/4 inch thick onto both ends of a 3-1/2 foot section of standard 6-inch pipe. A relief valve was installed on top of the mixing vessel. This relief valve provided a means of controlling the pressure in the system and also provided for the release of the steam condensate from the system. From the mixing vessel, the hot water flowed through an 8-foot section of straight 1-1/2 inch pipe in which the metering orifice was placed. From the metering orifice, the hot stream flowed to the suction side of the pump.

As a general rule, it is not advisable to place an orifice on the suction side of a centrifugal pump since cavitation might develop in the pump. This is particularly true when pumping a fluid near its boiling temperature. However, over a period of six months of operation, with a hot water pressure of 15 psig and hot water temperatures as high as 225°F, no cavitation within the pump was detected.

#### Temperature Measurement

Four temperatures were measured during the test runs.

These were the inlet and outlet temperatures of both the hot and cold streams. Two sets of four thermometers each were used for the temperature measurements. The set of thermometers used to obtain the Wilson plots were 24 inches long with a range of  $-1$  to  $+101^{\circ}\text{C}$  and were graduated in  $1/10^{\circ}\text{C}$  divisions. The set of thermometers used during the scaling runs were 24 inches long with a range of  $+30$  to  $+220^{\circ}\text{F}$  and were graduated in  $1/5^{\circ}\text{F}$  divisions. These eight thermometers were calibrated against a thermometer of known accuracy. The thermometer calibrations are plotted in Figures 22, 23, 24, and 25.

#### Flow Measurement

The flow rates of the hot and cold streams were measured with square-edged orifices. The orifice calibrations are shown in Figures 26 and 27. The orifice plates used in both systems were machined from  $1/16$ -inch steel plate. The diameter of the orifice used in the hot stream was 0.656 inches, and the diameter of the orifice used in the cold stream was 0.781 inches.

Two  $1\text{-}1/2$  inch black iron unions were modified to hold the orifice plates. The lips protruding from the male sides of both unions were removed, and a  $1/32$ -inch groove was cut into the flat faces to hold the orifice

plates. Matching  $1/32$ -inch grooves were also cut into the female sides of the unions to give an exact fit for the plates. Pressure taps were drilled  $7/16$  inch above and below the orifice plates. Suitable gasket material was used to assure a leak-proof connection. The orifice in the hot stream was placed so that there were 41 diameters of straight pipe above and 23 diameters of straight pipe below the orifice plate. There were 56 diameters of straight pipe above and 10 diameters of straight pipe below the cold stream orifice plate.

The manometers which measured the pressure drop across both orifices were the double differential type and contained water over mercury. Hence, the manometer fluid had an effective density of 12.56. Both manometers had a range of 32 inches.

## PROCEDURE

To begin a run, the cold stream circulation pump was started, and the cold stream flow was adjusted to the desired rate. Cold water was admitted to the cooling coils in the cold stream resaturation vessel. The steam valve to the hot stream was opened, and the hot stream circulation pump was started immediately afterwards. The hot side stream flow was adjusted to the desired rate. All manometer lines were cleared to assure they were free of air. The system was allowed one hour to come to equilibrium, and then data was taken until the end of a run.

To shut down, the cold water to the cooling coils was turned off, and the cold stream circulation pump was stopped. The steam supply to the hot side stream was shut off, and the hot stream circulation pump was stopped. After the system had cooled off, the finned tube was removed and replaced or cleaned for the next run.

The scaling runs for each of the finned tubes took from seven to ten days of continuous operation. Data was generally taken three times a day: between 8 and 9 AM, between 2 and 4 PM, and between 10 and 12 PM. The experimental data consisted of four temperature readings (hot and cold stream inlet and outlet temperatures) and two manometer readings (hot and cold stream flow rates).

The runs for each of the five Wilson plots lasted for one to two days of continuous operation. The same four temperature readings and two manometer readings as were taken for the scaling runs were noted every fifteen minutes. When the readings remained approximately constant, the system was considered to be in equilibrium at that flow rate. The flow rate was then changed, and the temperatures were noted until thermal equilibrium was again attained. The annular fluid velocity was varied from 2 to 10 feet-per-second for the Wilson plots.

Throughout the investigation, the experimental system ran very smoothly. The flow rates could be maintained within a range of  $\pm 0.3$  pounds-per-minute, and the temperatures rarely varied more than  $\pm 8^{\circ}\text{F}$  from the overall average temperature of a run. Since the steam used to heat the hot stream was taken directly from the campus steam supply, any large increase or decrease in steam demand anywhere in the campus system caused fluctuations in the steam flow rate to the experimental apparatus. Under these conditions, a variation in the hot steam temperatures of only  $8^{\circ}\text{F}$  from the average temperature of a whole run was considered good. However, since the fluctuations in the steam supply would throw the experimental system out of thermal equilibrium for a short period of time, data taken during

these periods would not be consistent with that taken under equilibrium conditions. Since the heat balances, and hence the overall heat transfer coefficients, were determined from comparatively small temperature differences, the non-equilibrium condition is easily detected in the calculated coefficients.

For the Wilson plots, it was possible to plot the experimental data before the completion of a run, and any points which seemed to be out of line were rerun under equilibrium conditions. Thus, there are double points at some velocities on the Wilson plots. However, since the conditions during a scaling run are a function of time, it was not possible to rerun any of these points. Therefore, it has been necessary to interpolate curves through regions of scattered data in a manner which seemed best from the knowledge of the system and of the general scaling behavior.



## DISCUSSION

Scale Formation on the Finned Tubes

To insure that a representative type of scale was used in this investigation, a literature search was carried out to determine the major constituents of hard water scales deposited during industrial heat transfer operations. Partridge's study of scale formation on boiler tubes presents a selection of hard water scales which have been deposited in industrial heat transfer operations (6, p.37). Of 15 scale samples that Partridge analyzed, calcium sulphate was a major constituent of six and was a minor constituent of seven more. Therefore, since calcium sulphate was present in thirteen of these fifteen scales and since it has an inverse solubility throughout the temperature ranges used in this study (Figure 16), calcium sulphate was the scaling salt used in this investigation.

Figures 6, 7, 8, and 9 are scaling plots with the overall heat transfer coefficient plotted as a function of time for the 5, 7, 9, and 19 fin/inch transverse finned tubes. The flow rates and temperatures of both streams flowing through the experimental apparatus were maintained approximately constant throughout each scaling run. Therefore, any decrease in the overall heat transfer coefficient during a run is due to the added resistance of the

deposited scale.

An examination of the scaling plot for the 5 fin/inch tube shows a definite drop in the overall heat transfer coefficient and indicates that scaling has occurred.

An examination of the scaling plot for the 9 fin/inch tube shows that the overall coefficient did not decrease but increased by approximately 19% of its original value. This definitely indicates that no scale was deposited.

Examination of the scaling plot for the 7 fin/inch tube shows a drop in the overall coefficient until the middle of the sixth day which indicates that scaling has occurred up to this time. However, during the sixth day, there is a sudden rise in the overall coefficient indicating a possible removal of some of the scale. This sudden rise was caused by a change in the conditions of the streams flowing through the experimental exchanger. At the start of this run, the temperature of the hot stream was higher than that of the other three runs. After six days of running at these higher hot side temperatures, it was decided that the run would be more informative if its temperatures were in line with those of the other three runs. Therefore, the steam supply to the hot stream was sharply reduced, and the temperatures returned to the desired level. Evidently the scale which had formed on the

FIGURE 6  
SCALING PLOT FOR THE 5 FIN/IN TUBE

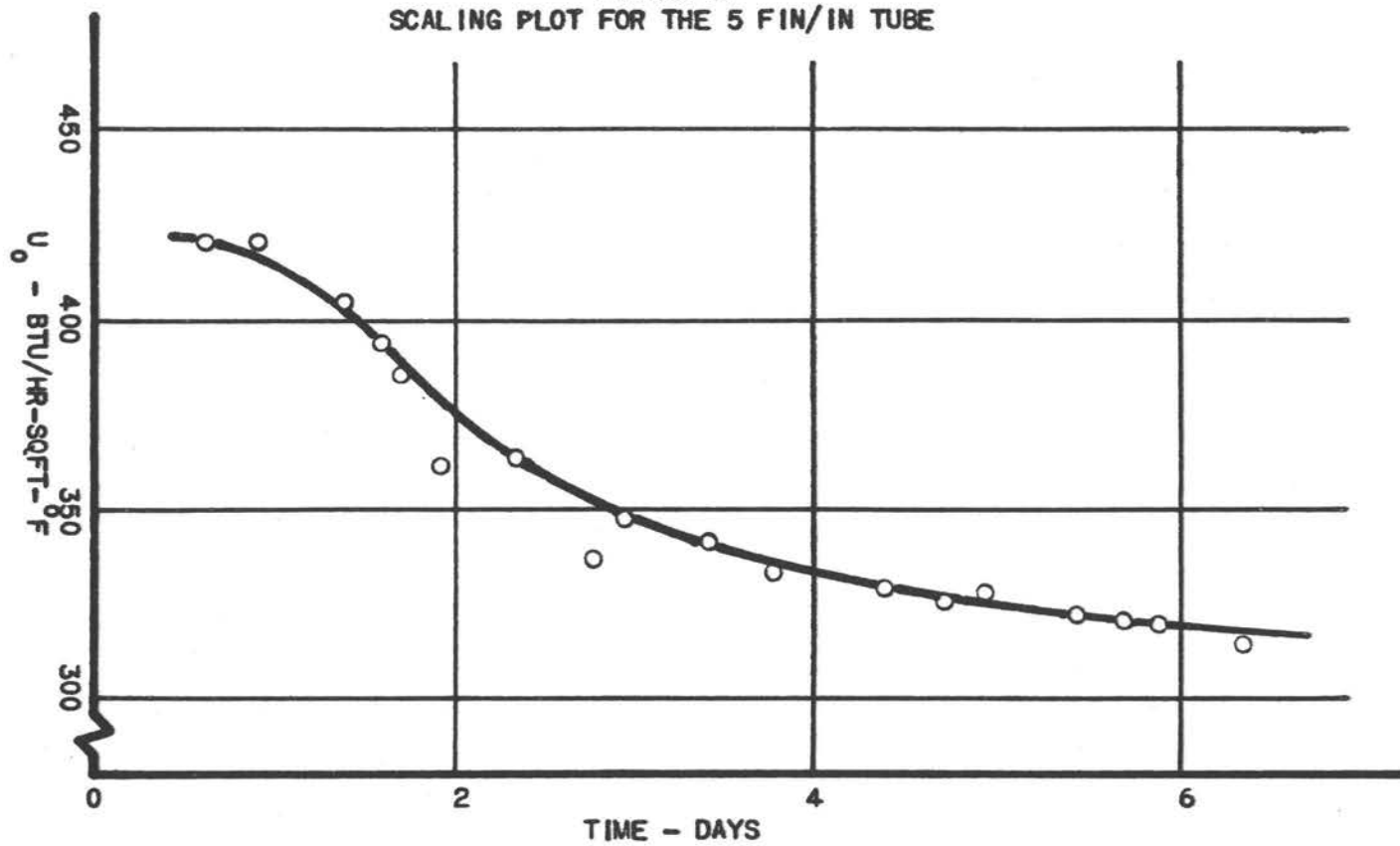


FIGURE 7  
SCALING PLOT FOR THE 7 FIN/IN TUBE

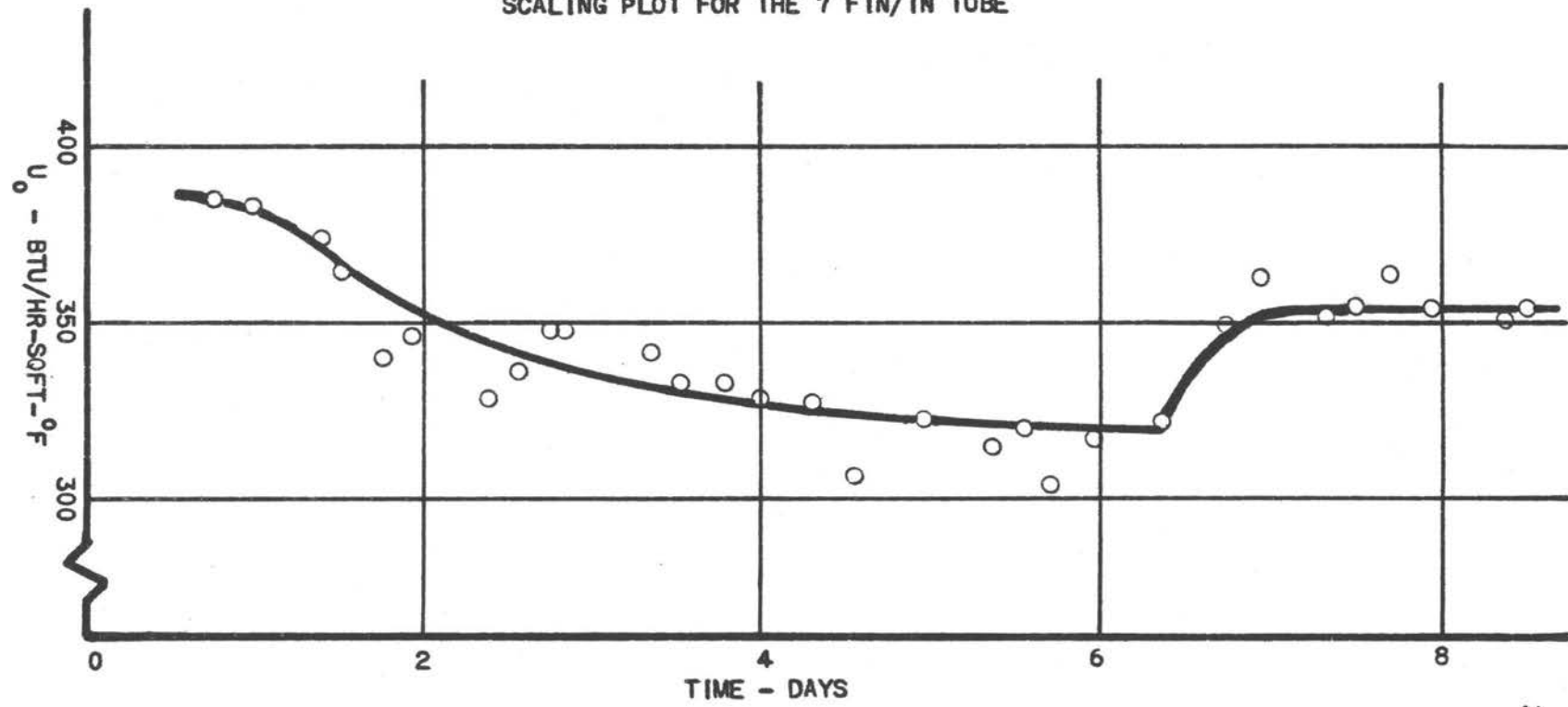


FIGURE 8  
SCALING PLOT FOR THE 9 FIN/IN TUBE

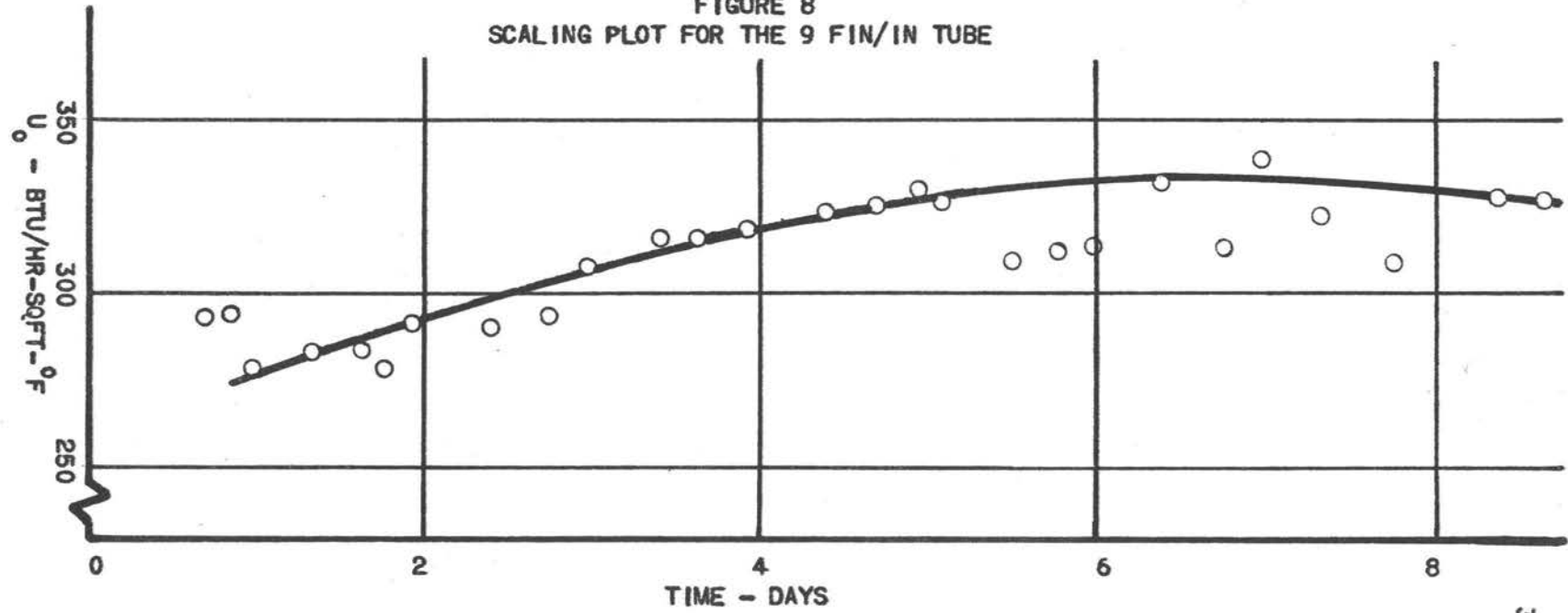
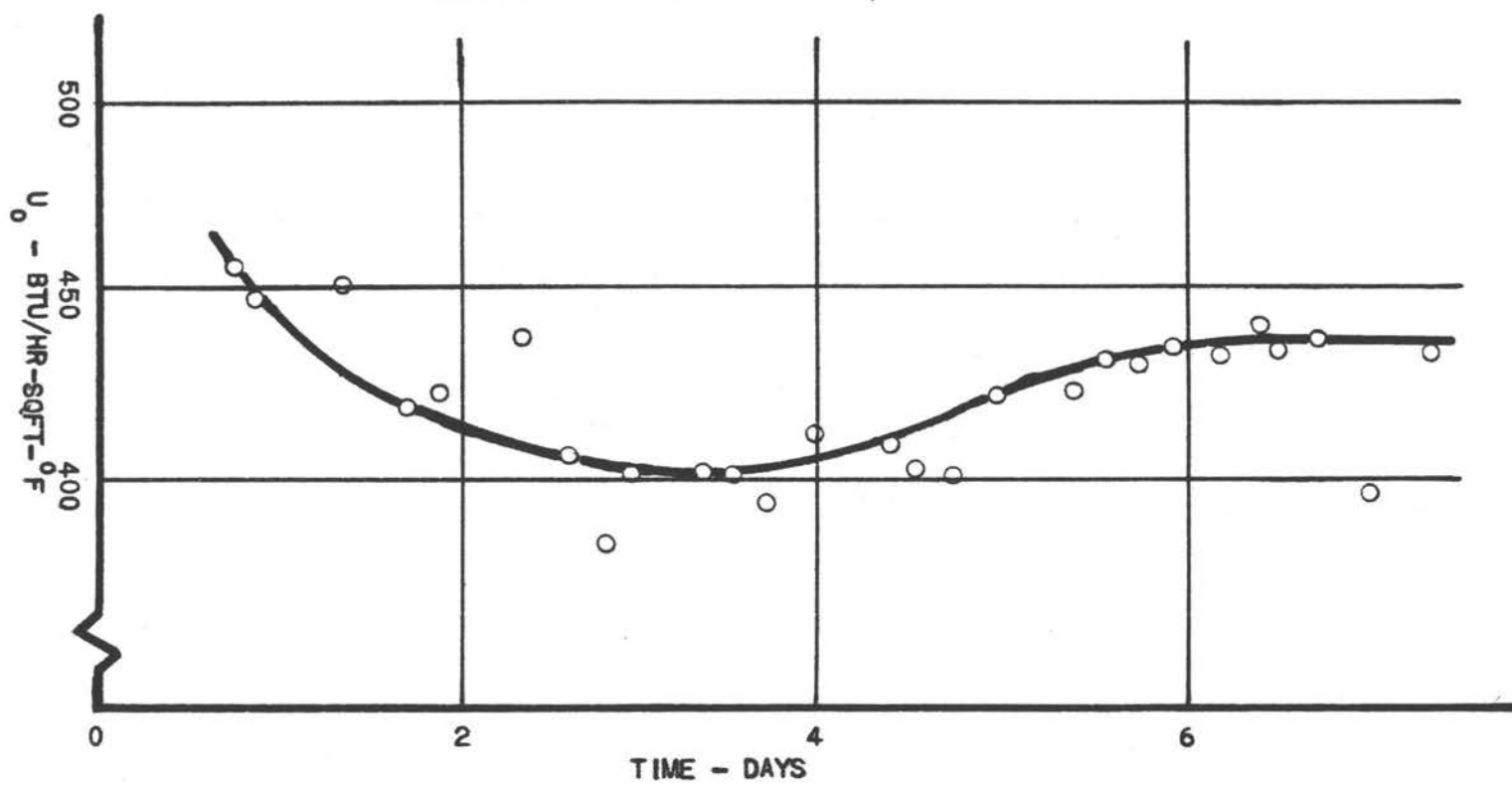


FIGURE 9  
SCALING PLOT FOR THE 19 FIN/IN TUBE



tube was removed in some manner, for the overall heat transfer coefficient rose to within 6% of its original value. This indicates that in the same temperature range as used for the three previous tubes, no scale would deposit on this tube.

An examination of the plot for the 19 fin/inch tube shows a gradual decrease in the overall heat transfer coefficient for the first three days and then a gradual increase in the coefficient for the next three days. At this time, the plot levels off at a constant value. This would indicate that there was some scale formation until the end of the third day but that the scale slowly redissolved, for some reason, from the third to the sixth day. From the sixth day, the scale deposit remained constant.

On first observation, there seems to be no relation in the scaling behavior of the four tubes. However, to attempt a correlation of the scaling behaviors, the mechanism of scale deposition should be considered.

Partridge's scaling mechanism for plain tubes is adaptable to the finned tube situation. He concluded that the formation of a scale deposit from hard water below its boiling temperature occurs through spontaneous crystallization of an inversely soluble salt or salts from the comparatively high temperature film layer adjacent to the

to the tube outer wall.

Knudsen and Katz studied the behavior of turbulent fluid flow along transverse finned tubes with various ratios of fin height to fin spacing (4, pp.490-500). They observed that eddies were formed between the fins under turbulent flow conditions and that different ratios of fin height to fin spacing caused different types and numbers of eddies to develop (Figure 10).

It is reasonable to expect that these eddies between the fins would considerably reduce the thickness of the laminar sublayer adjacent to the fins. Since Partridge concluded that scale is deposited from this laminar sublayer, the type of flow between the fins will probably effect the amount of scale which can be deposited.

Knudsen and Katz's investigation shows that for a W/S ratio of 0.76 to 1.35 a single eddy develops between the fins and that for a W/S ratio of 1.95 to 2.2 two circular eddies develop between the fins. Their investigation also shows that as the W/S ratio approaches 1.35 the single circular eddy becomes elongated. It is probable that a transition from the single elongated eddy to the two eddy formation occurs at a W/S ratio between 1.35 and 1.95.

It might be expected that the double eddy formation would more completely fill the space between the fins



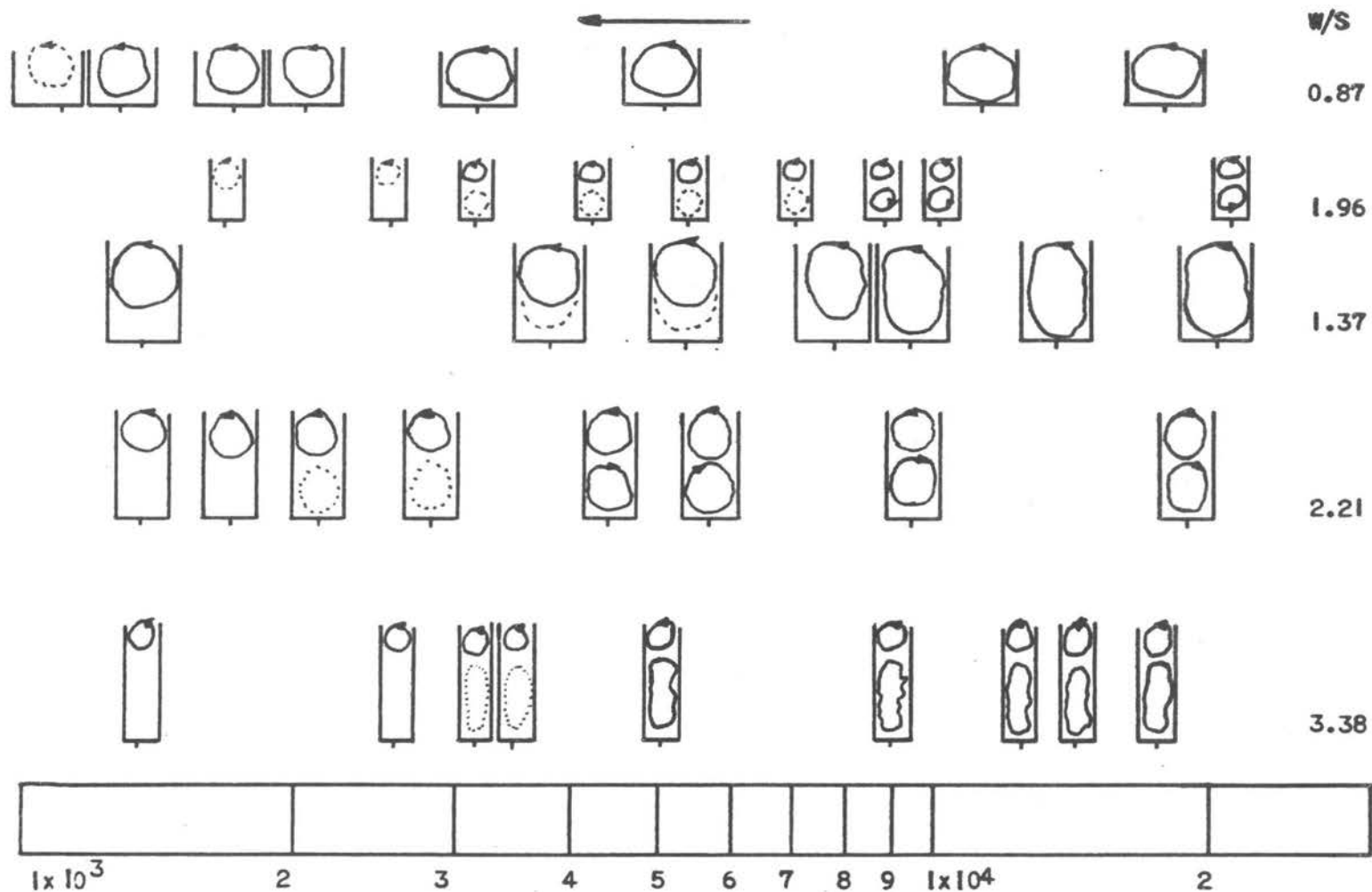


FIGURE 10 - SKETCH OF FLOW PATTERNS DEVELOPED BETWEEN THE FINS

with turbulent fluid than would the single elongated eddy condition. Hence, it would also tend to reduce the thickness of the laminar sublayer to a greater extent. Since very little supersaturated fluid would be at the tube surface, very little scale would be deposited. The W/S ratios of the 5, 7, 9, and 19 fin/inch tubes are 1.42, 2.01, 2.58, and 1.56 respectively. This would indicate that the 5 fin/inch tube would have a single, elongated eddy between its fins; that the 7 and 9 fin/inch tubes would have double eddies between their fins; and that the 19 fin/inch tube, being in the transition range, might have either one or two eddies between its fins.

The scaling plot of the 9 fin/inch tube shows an increase in the overall heat transfer coefficient which indicates that no scale has been deposited. The scaling tests on the 7 fin/inch tube were at first conducted at higher tube temperatures than those used for the other three tubes. The immediate increase in the overall heat transfer coefficient as soon as the temperatures were reduced to those of the other tubes indicates that the scale was redissolved or removed from the tube surface. The final overall coefficient after several days of running at the reduced temperatures was only 6% below the initial coefficient. This could be due to baking of the scale

onto the tube at the higher temperatures so that it would not redissolve into the water stream; so it is concluded that the 7 fin/inch tube did not scale. Therefore, the data from these two tubes agrees with the assumption that the double eddy formation almost completely removes the scale forming laminar sublayer next to the fins and hence decreases scale deposition.

If it is assumed that the elongated single eddy formation between the fins would not affect the laminar sublayer as completely as the two eddy formation, one would expect that more scale would be deposited, particularly at the sharp corners where the fin joins the tube. An examination of the scaling plot for the 5 fin/inch tube, the tube with the single elongated eddy formation, shows a distinct drop in the overall heat transfer coefficient and definitely indicates that scale has been deposited.

An examination of the scaling plot for the 19 fin/inch tube shows a drop in the overall coefficient for the first three days, and an increase for the next three days, after which it levels off at an overall coefficient which is only 4.5% below the initial coefficient. This would indicate that there was almost no scale formation on the tube by the end of the run. Since the W/S ratio for this tube lies in the transition region between the

one and two eddy formation, it is postulated that for the first three days there was a single eddy between the fins and scale was deposited. But for some reason, two eddies developed between the fins during the third day, and the scale deposit slowly redissolved until an equilibrium was obtained for the two eddy situation. There was a  $10^{\circ}\text{F}$  increase in the cold stream temperature at the middle of the third day which might have decreased the viscosity sufficiently to allow a change from the one to two eddy behavior.

At the end of the scaling run for each tube, the tube was removed from the experimental exchanger and allowed to dry for several days. The scale deposit on the tubes was observed, and the scale deposit on a representative area of the tube was removed and weighed.

All four of the tubes investigated had some scale deposited in the sharp corners at the base of the fin where the fin joins the tube. For the 7, 9, and 19 fin/inch tubes, this was the only place where scale was found. For the 5 fin/inch tube, the scale deposit was spread uniformly over the fins and tube surface, but there was a particularly heavy deposit at the base of the fins. The scale deposit from a 10-inch length of each tube was carefully removed, collected and weighed on an analytical

balance accurate to 0.0001 grams. Table II shows the amount of scale found on each tube.

The scale on the 19 fin/inch tube was particularly hard to remove because of the small spacing between the fins. Hence, the value of 0.000021 lb/sqft may be somewhat low.

It can be seen that the weights of the scale deposits shown in Table II are in agreement with the scaling plots on the four finned tubes. They show that there was very little scale deposited on the 7, 9, and 19 fin/inch tubes and that there was a much larger scale deposit on the 5 fin/inch tube.

Therefore, it is indicated by this investigation that under moderate scaling conditions the amount of scale deposit on a transverse finned tube is a function of the flow patterns between the fins. When the two eddy formation develops between the fins, there is considerably less scale deposited on a tube than there is when a single elongated eddy develops.

TABLE II

## WEIGHT OF SCALE DEPOSITED ON THE FINNED TUBES

Tube	Weight of Scale Deposited
5 fin/inch	0.000230 lb/sqft finside surface
7 "	0.000070 "
9 "	0.000031 "
19 "	0.000021 "

Conditions:	Tube:			
	5 f/in	7 f/in	9 f/in	19 f/in
Ave. temp. of hot stream - °F	192.6	185.2	175.3	183.0
Ave. temp. of cold stream - °F	144.9	138.1	132.9	139.8
Ave. velocity of hot stream - ft/sec	24.30	22.92	22.74	6.41
Ave. velocity of cold strm. - ft/sec	4.08	3.56	3.41	3.39

### Correlation of the Finside Heat Transfer Coefficients

Figure 11 shows the experimentally determined effective outside heat transfer coefficient plotted as a function of the annular fluid velocity. Curves of similar data obtained by Knudsen and Katz (4, pp.490-500) are also included. It can be seen that all of the curves have similar slopes. In Figure 12 the experimental data are plotted according to equation (4) where

$$Nu/(Pr)^{0.4}(S/D_e)^{0.4}(W/D_e)^{-0.19}$$

is plotted versus the Reynolds number. Since an individual curve is obtained for each tube, no correlation is apparent.

Since a correlation was not obtained with equation (4), an analysis was carried out to determine whether or not a change in the exponents of the dimensionless groups or the addition of another dimensionless group to the equation would bring the two sets of data together. However, no correlation could be developed.

Reference was then made to the experimental work of Knudsen and Katz, and it was found that the two sets of data were taken under different conditions.

In their investigation of the effect of annular fluid velocity on the effective outside heat transfer coefficient, they held the velocity of the annular fluid

FIGURE 11  
EFFECTIVE FINSIDE FILM COEFFICIENT  
VS ANNULAR FLUID REYNOLDS NUMBER

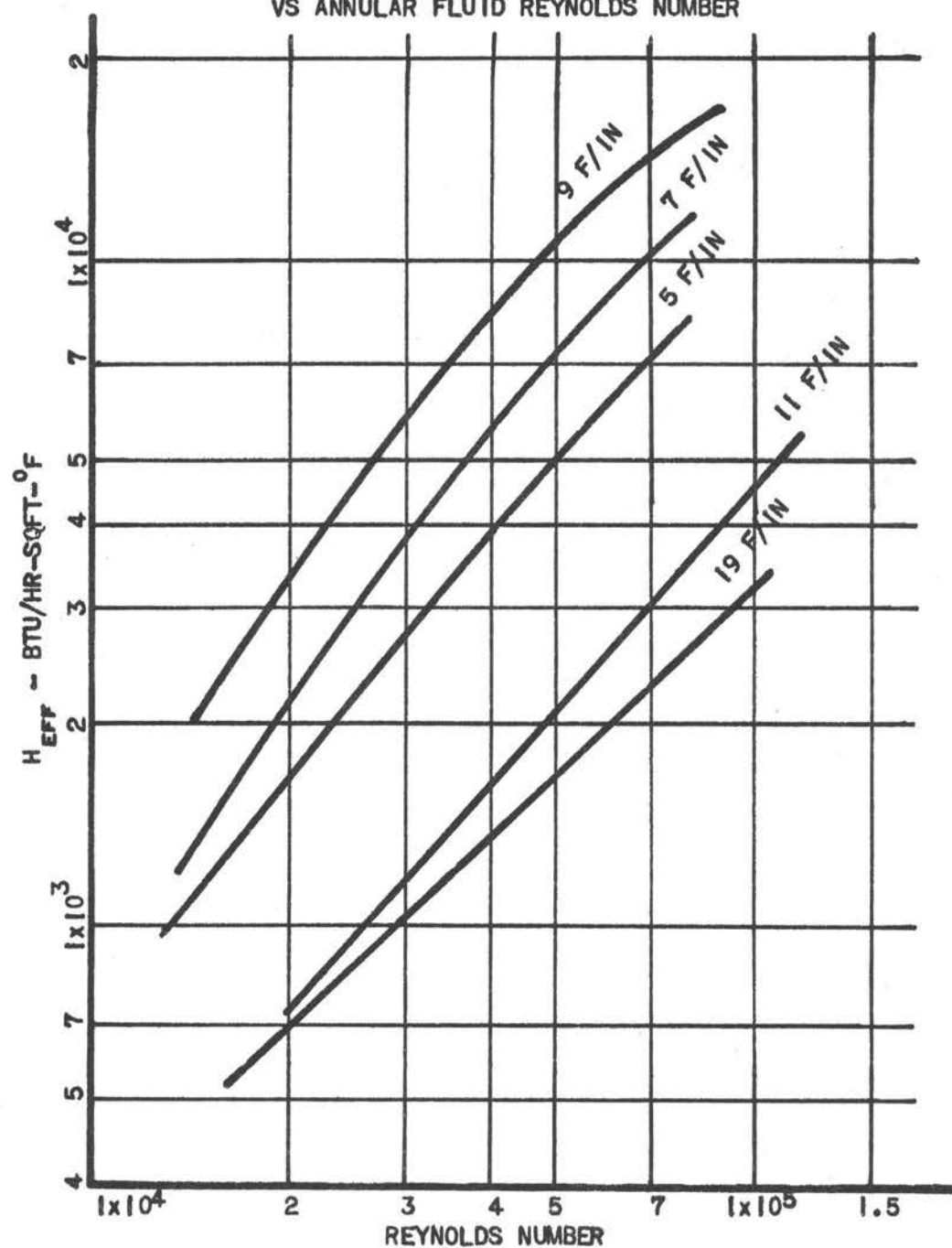
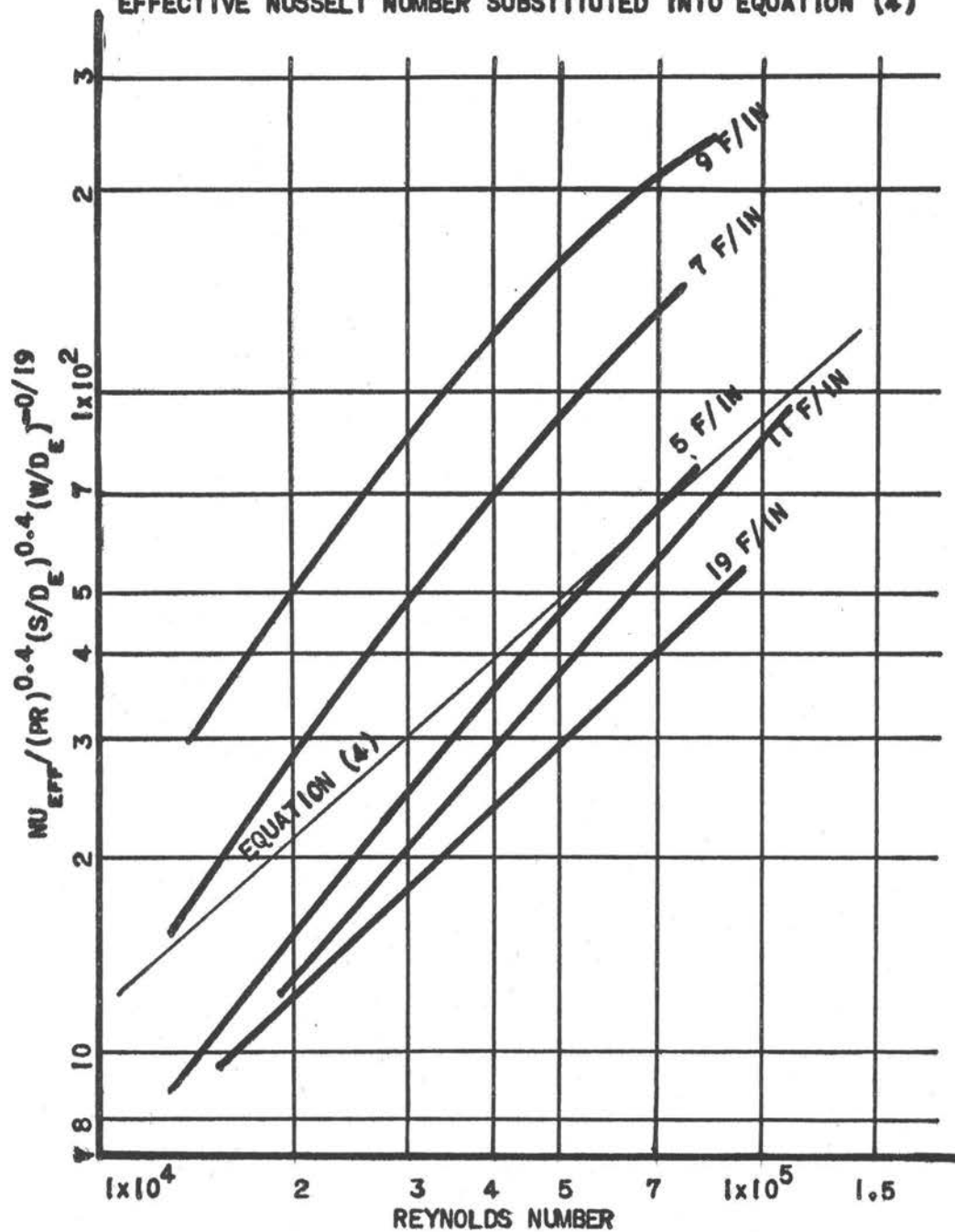




FIGURE 12

EFFECTIVE NUSSELT NUMBER SUBSTITUTED INTO EQUATION (4)



constant and varied the velocity of the fluid within the inner tube of the annulus. From the Wilson plot obtained it was possible to calculate the inside heat transfer coefficient and the inside film resistance at any inner fluid velocity. Knowing the thickness of the tube wall, it was easy to calculate the resistance to heat transfer caused by the wall. Then using the relation

$$1/U_o = R_o = R_{is} + R_w + R_{os} \quad (7)$$

it was simple to calculate the apparent outside heat transfer coefficient. Using the Gardner (1, pp.621-631) fin efficiency, the apparent heat transfer coefficient was corrected for the effective area.

In the present study, however, somewhat different conditions were used to obtain the apparent outside heat transfer coefficient. In order to determine the effect of the annular fluid velocity on the outside heat transfer coefficient, the velocity and temperature of the inside fluid was held constant, and the velocity of the annular fluid was varied. For a constant inside fluid velocity and fluid temperature,  $R_{is}$  and  $R_w$  are constant. Therefore, the apparent outside coefficient may be easily determined from the relation:

$$1/U_o = R_o = C + R_{os} = C + 1/h_{os} \quad (8)$$

Then the Gardner fin efficiency was employed to correct

the apparent film coefficient for the effective fin area.

However, the Gardner fin efficiency is a function of the heat transfer rate as well as of the dimensions of the finned tube. As the velocity of the annular fluid, and also the heat transfer rate, was varied, the fin efficiency, and hence the effective area, also varied. Therefore, due to these different methods used to obtain the Wilson plot data, the experimental findings of Knudsen and Katz and those of this study are not compatible; and a correlation could not be developed between the two.

The data from this study was analyzed in a manner similar to that used by Knudsen and Katz to obtain a general correlation, but there was not enough data to determine the empirical constants. Hence, the data from this study is presented in Figures 13 and 14 plotted as the apparent outside heat transfer coefficient. It is felt that even if a correlation of the data from this study could have been developed, it would have been of limited value, for the variation of fin efficiency which occurs with a variable annular fluid velocity is very difficult to determine.

FIGURE 13  
APPARENT FINSIDE FILM COEFFICIENT  
VS ANNULAR FLUID REYNOLDS NUMBER

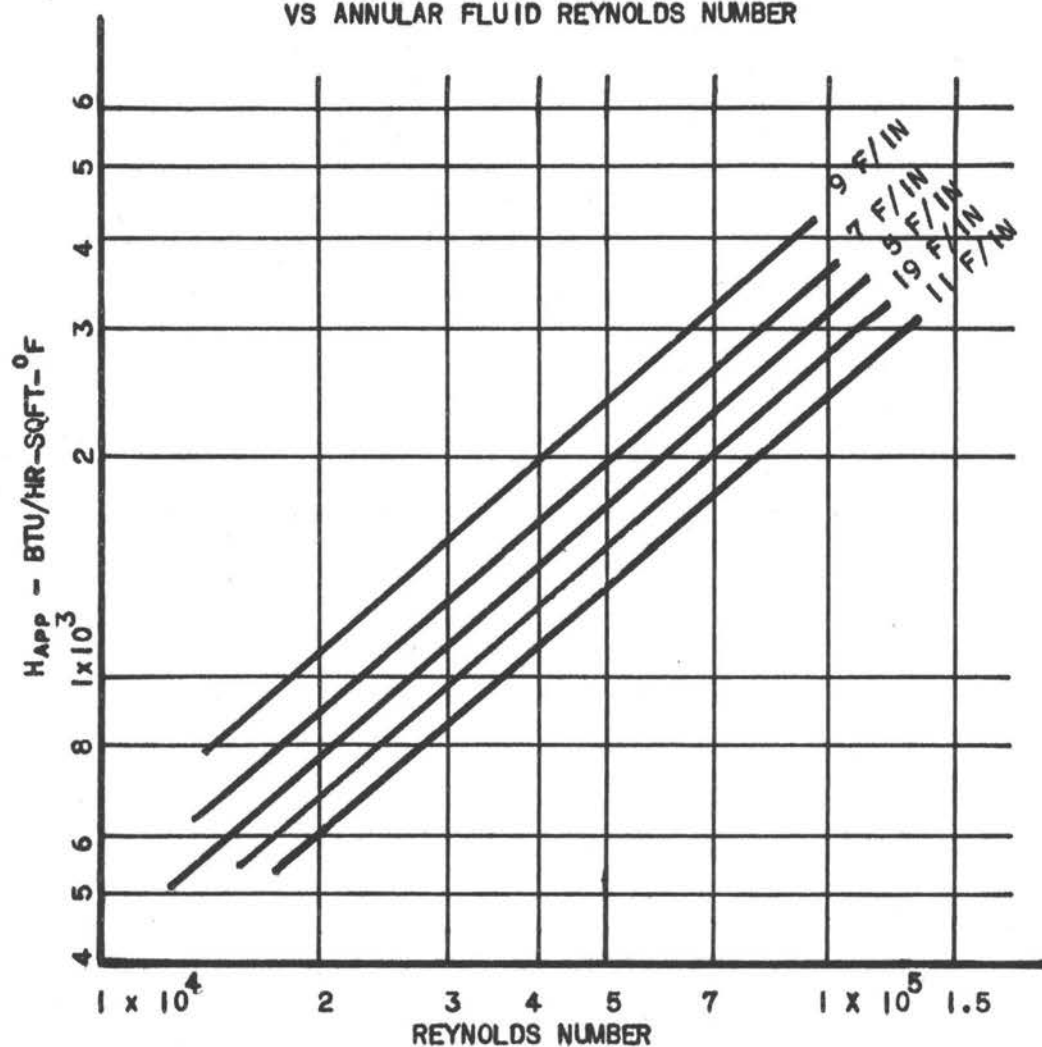
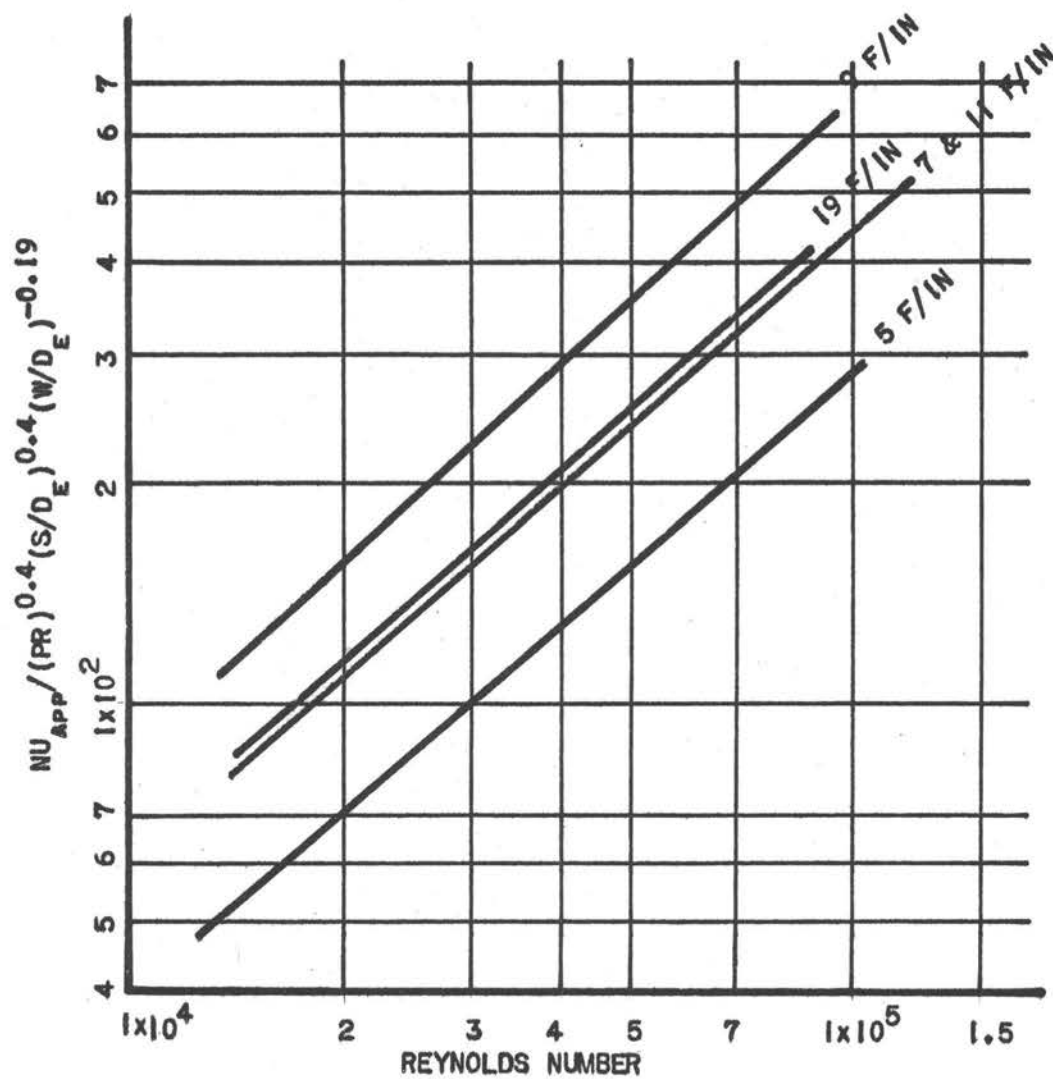


FIGURE 14  
APPARENT NUSSELT NUMBER SUBSTITUTED INTO EQUATION (4)



Comparison of the Experimental Scaling Factors to those Recommended by the Tubular Exchanger Manufacturers Association.

The fouling factor,  $f$ , is determined from the following equation (5, p.188):

$$f = 1/h_s = 1/U_s - 1/U \quad (9)$$

where  $h_s$  is the film coefficient from the scale,  $U$  is the overall coefficient from the tube when it is clean, and  $U_s$  is the overall coefficient from the tube when it is scaled.

Figure 15 is a plot of the fouling factor,  $f$ , as a function of time for the 5 fin/inch tube. The Figure also shows the  $f$  value recommended by the Tubular Exchanger Manufacturers Association for plain tubes operating in hard water (8, p.49). The three lowest overall coefficients measured during the scaling period of the run on the 7 fin/inch tube have been included for an additional fin tube-plain tube comparison.

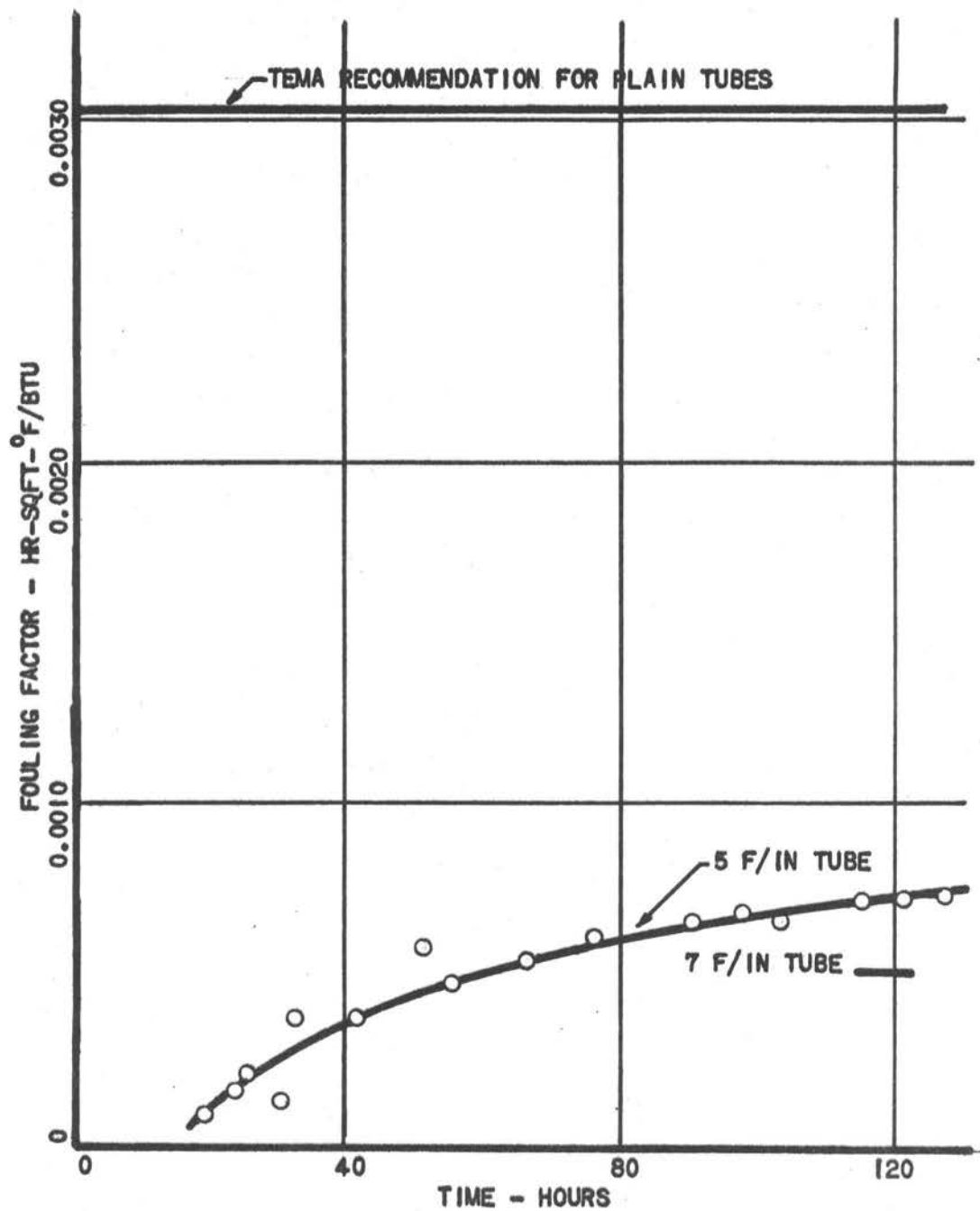
It is apparent from Figure 15 that the fouling factors for the 5 and 7 fin/inch tubes are considerably less than those recommended by the Tubular Exchanger Manufacturers Association for plain tubes. It is also apparent that the two eddy formation which developed between the fins of the 7 fin/inch tube resulted in less scaling

than did the single elongated eddy formation which developed on the 5 fin/inch tube.

Katz, et al., (3, pp.123-125) studied the fouling characteristics of identical plain and transverse finned tube bundles used to heat bunker C fuel oil. They also found that the fouling factor for transverse finned tubes was less than that for plain tubes when both operated under the same fouling conditions.

It is possible that the Tubular Exchanger Manufacturers Association recommended fouling factors are somewhat higher than the industrial average to include the worst scaling which might develop within the general scaling classifications they list. However, the finned tube fouling factors determined in the present investigation are considerably less than those recommended by the Tubular Exchanger Manufacturers Association. Therefore, for the moderate scaling conditions studied, it is concluded that the use of the fouling factors recommended by the Tubular Exchanger Manufacturers Association for design utilizing transverse finned tubes is a conservative design procedure.

FIGURE 15  
COMPARISON OF EXPERIMENTAL AND TEMA RECOMMENDED FOULING FACTORS





## RECOMMENDATIONS

It is recommended that further investigation of the scaling characteristics of transverse finned tubes be carried out under more stringent scaling conditions. Such conditions could be attained using the present experimental apparatus with the following modifications:

1. Increased temperatures of the hot side fluid through higher pressures on the hot water system or through substituting steam for hot water in the hot stream system. An independent steam supply or the use of a higher pressure steam supply to the steam injector would facilitate maintaining higher temperatures.

2. Increased temperatures of the cold side fluid by enclosing the resaturation vessel and pressurizing the cold stream system.

It is felt that increasing the temperatures on the cold side stream are particularly important since scaling was not achieved until the maximum practical temperatures available with the present system were used.

It is recommended that further investigation be carried out to more completely determine the effect of the eddy formation between the fins on the scaling characteristics of a transverse finned tube. Further investigation of the Reynolds number at which the one eddy

situation transposes to the two eddy situation is also recommended.

It is recommended that other fouling media be investigated to more completely compare the performance of a transverse finned tube with that of a plain tube under various fouling conditions.

## CONCLUSIONS

The following conclusions result from this investigation:

1. For the moderate scaling conditions studied, the fouling factors recommended by the Tubular Exchanger Manufacturers Association may be used for design calculations involving transverse finned tubes.

2. A transverse finned tube with a  $W/S$  ratio which causes two eddies to develop between the fins will have a lower scaling factor under the same heat transfer and scaling conditions than will a transverse finned tube with a  $W/S$  ratio which causes a single elongated eddy to develop between the fins.

3. A general equation to relate the finned side film coefficient of a transverse finned tube to the velocity and properties of the fluid flowing past the tube can not be obtained from this investigation. The experimental method of Knudsen and Katz is a better method for obtaining the data required to develop such an equation.

## BIBLIOGRAPHY

1. Gardner, Karl A. Efficiency of extended surfaces. Transactions of the American society of mechanical engineers 67:621-631. 1945.
2. National research council. International critical tables of numerical data, physics, chemistry and technology. Vol. 1. New York, McGraw-Hill, 1928. 481p.
3. Katz, Donald L. et al. Fouling of heat exchangers. Petroleum refiner 33:123-125. August, 1954.
4. Knudsen, James G. and Donald L. Katz. Heat transfer and pressure drop in annuli. Chemical engineering progress 46:490-500. 1950.
5. McAdams, William H. Heat transmission. 3d ed. New York, McGraw-Hill, 1954. 532p.
6. Partridge, Everett P. Formation and properties of boiler scale. Ann Arbor, University of Michigan, 1930. 170p. (Michigan. University. Engineering research institute. Engineering research bulletin no. 15)
7. Rothfus, R. R., C. C. Monrad, and V. E. Senecal. Velocity distribution and fluid friction in smooth concentric annuli. Industrial and engineering chemistry 42:2511-2520. 1950.
8. Tubular exchanger manufacturers association. Standards of the tubular exchanger manufacturers association. 2d ed. New York, 1949. 93p.
9. Wilson, E. E. A basis for rational design of heat transfer apparatus. Transactions of the American society of mechanical engineers 37:47-82. 1915.

## APPENDIX

FIGURE 16

SOLUBILITY OF CALCIUM SULPHATE IN WATER VS TEMPERATURE

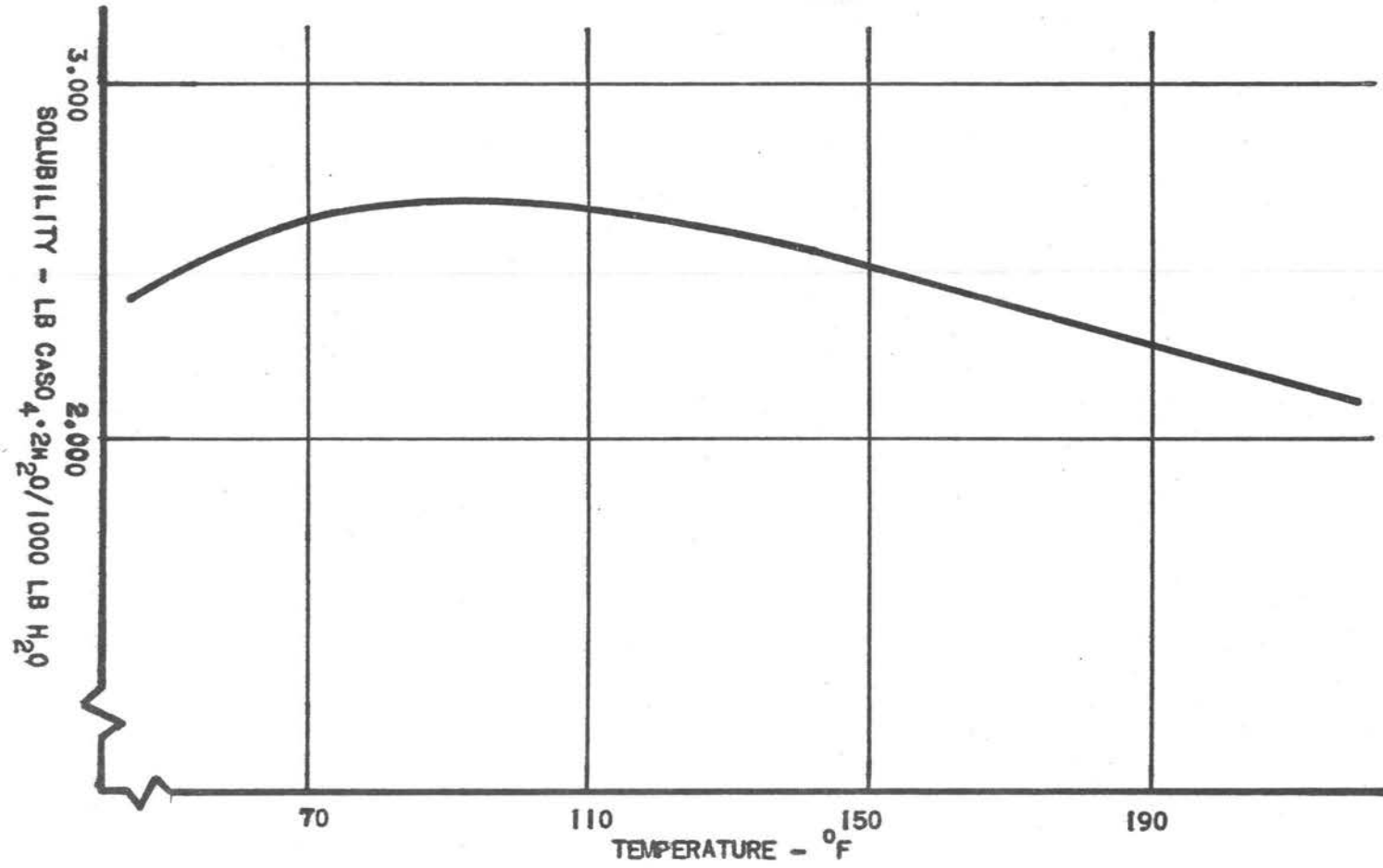


FIGURE 17  
WILSON PLOT FOR THE 5 FIN/IN TUBE

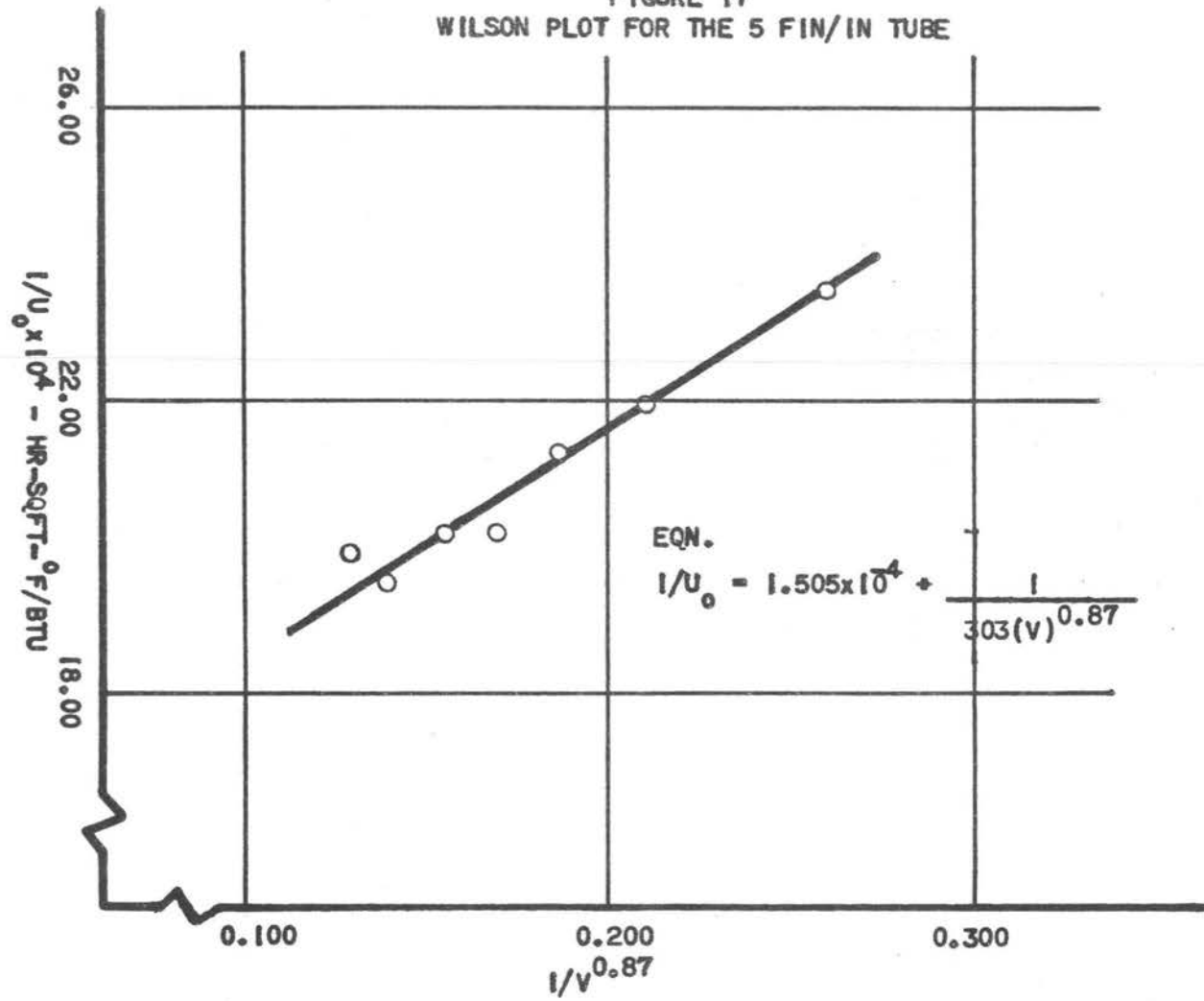


FIGURE 18

WILSON PLOT FOR THE 7 FIN/IN TUBE

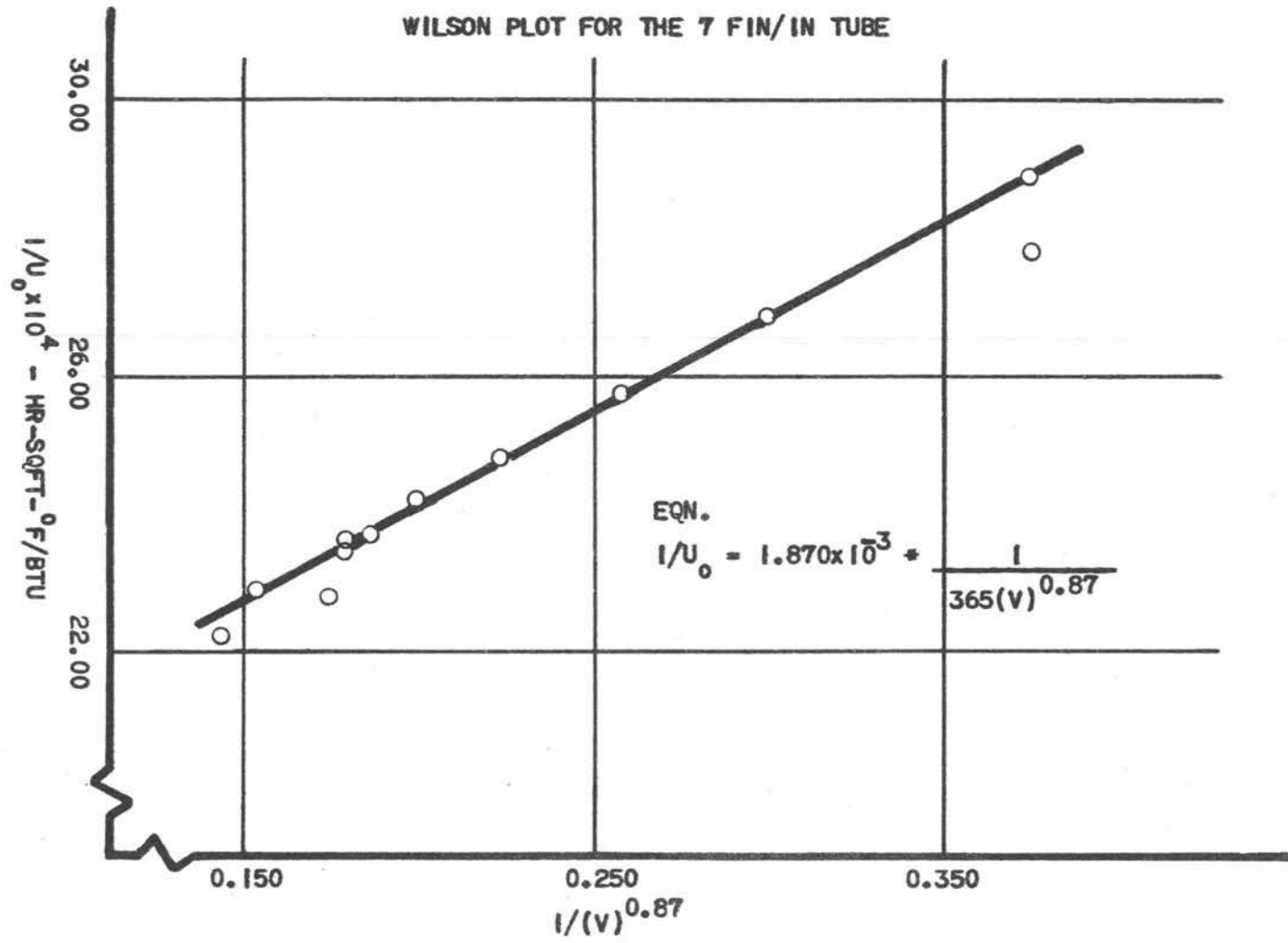




FIGURE 19  
WILSON PLOT FOR THE 9 FIN/IN TUBE

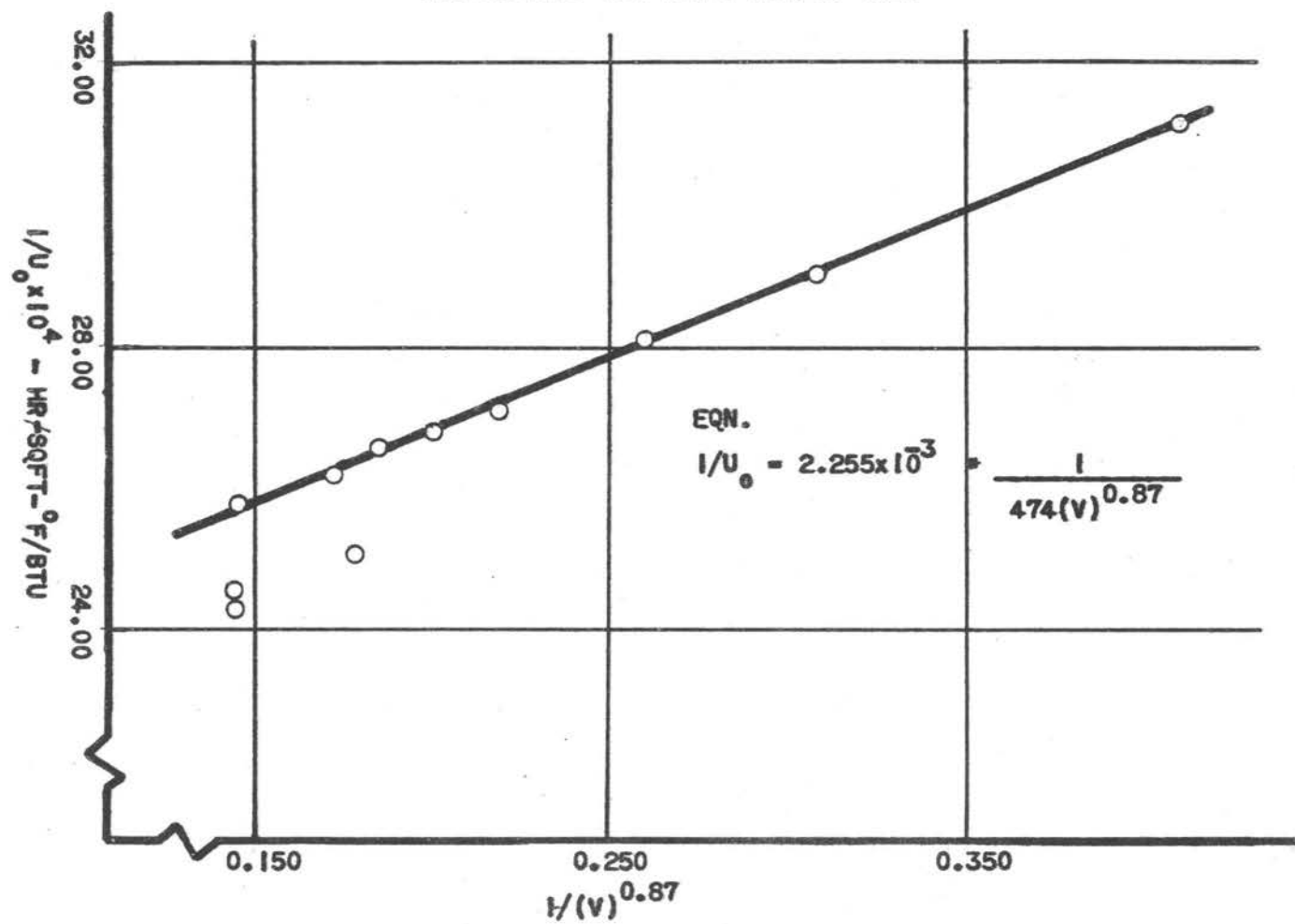


FIGURE 20  
WILSON PLOT FOR THE 11 FIN/IN TUBE

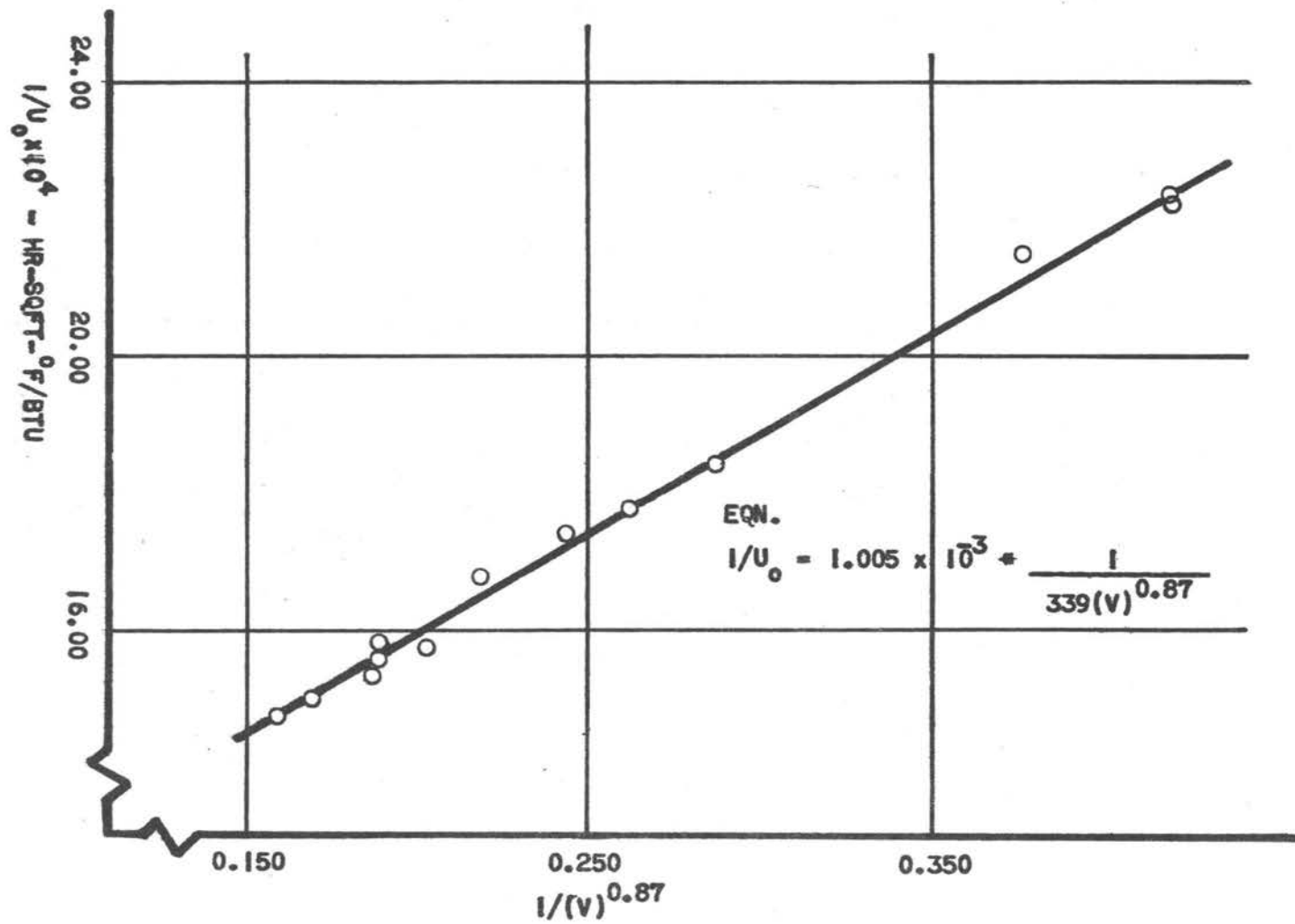


FIGURE 21

WILSON PLOT FOR THE 19 FIN/IN TUBE

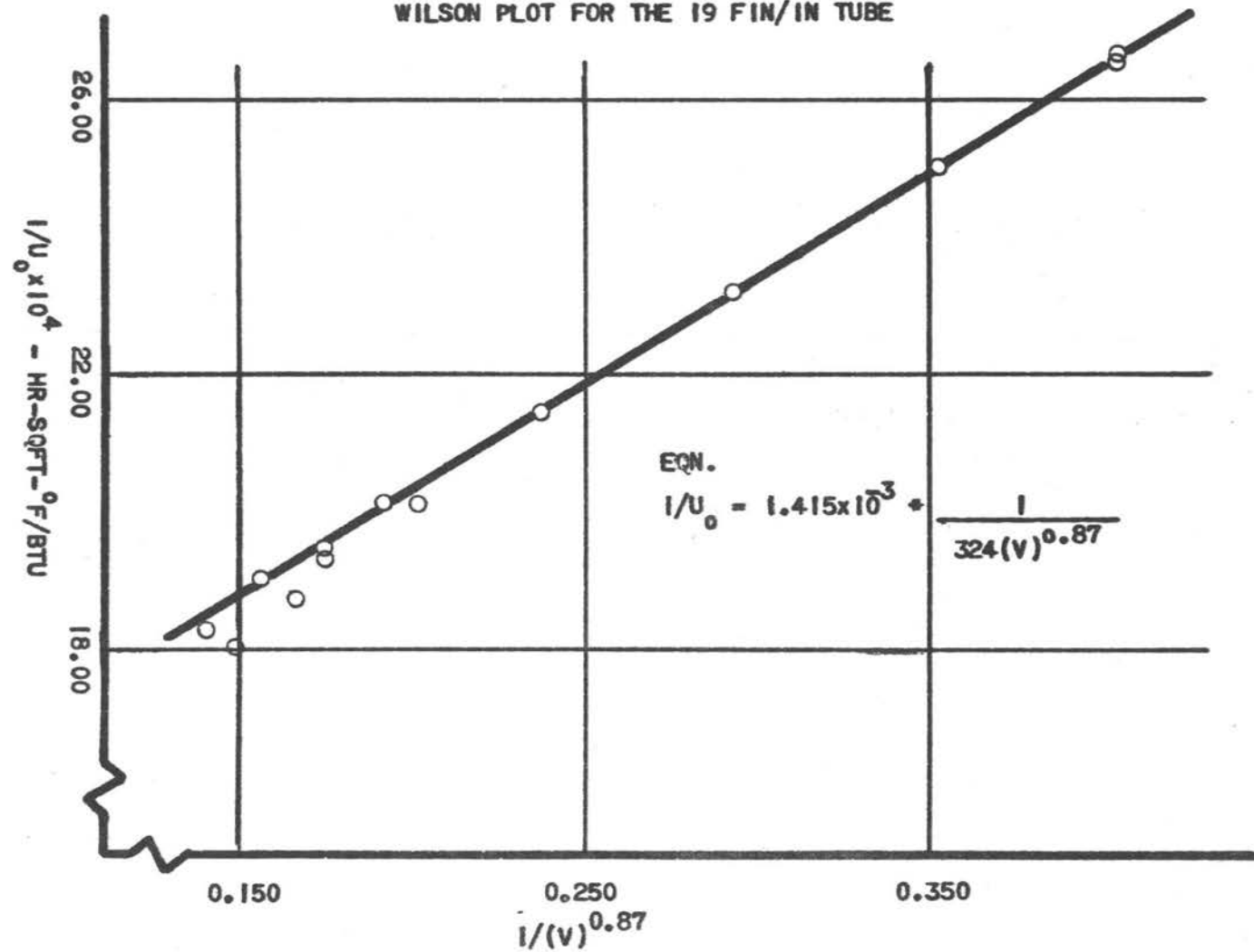


FIGURE 22

CENTIGRADE THERMOMETER CALIBRATIONS

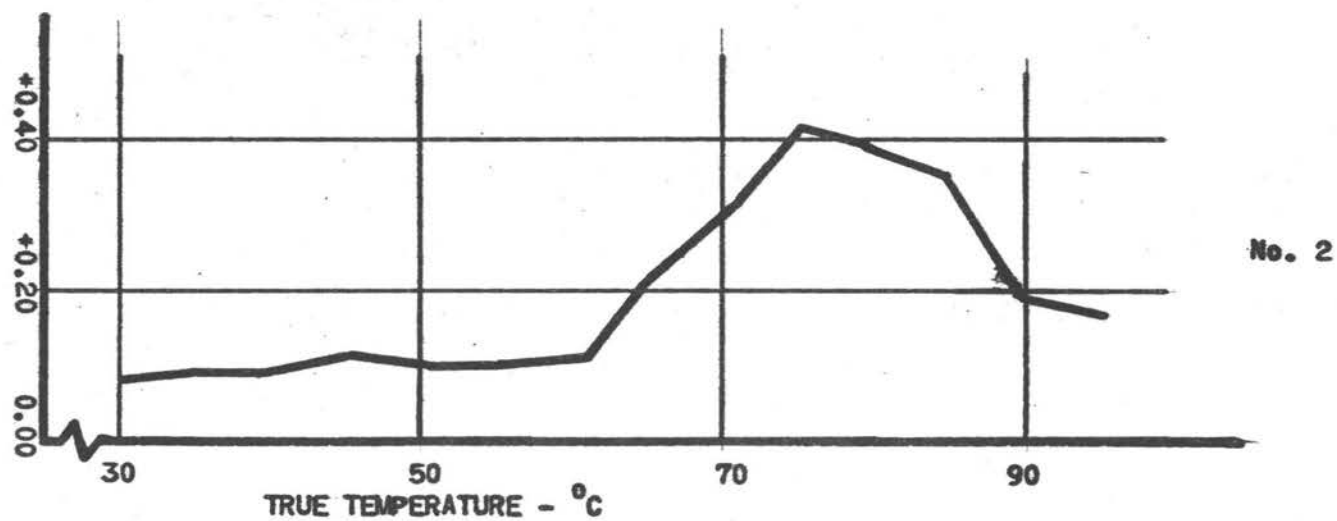
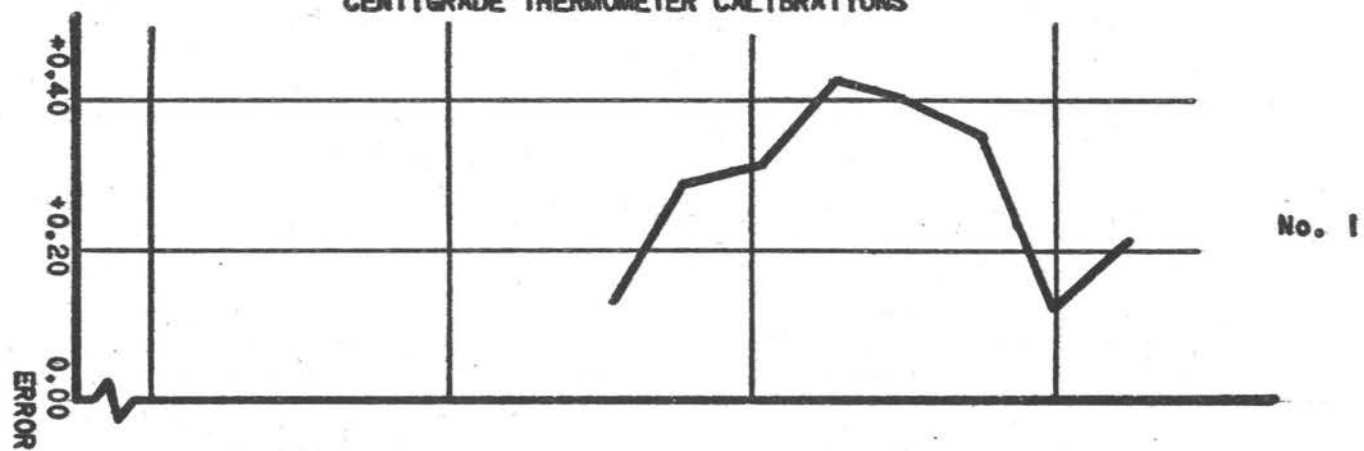


FIGURE 23  
CENTIGRADE THERMOMETER CALIBRATIONS

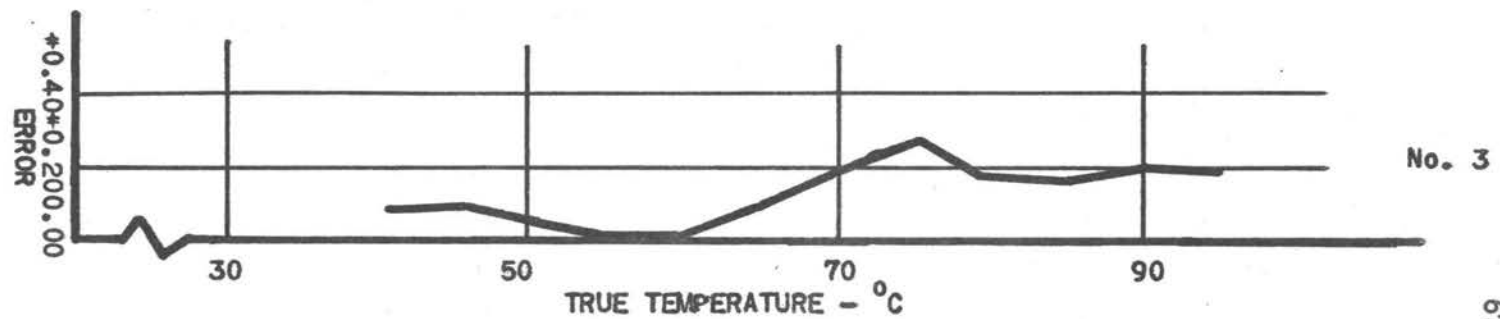
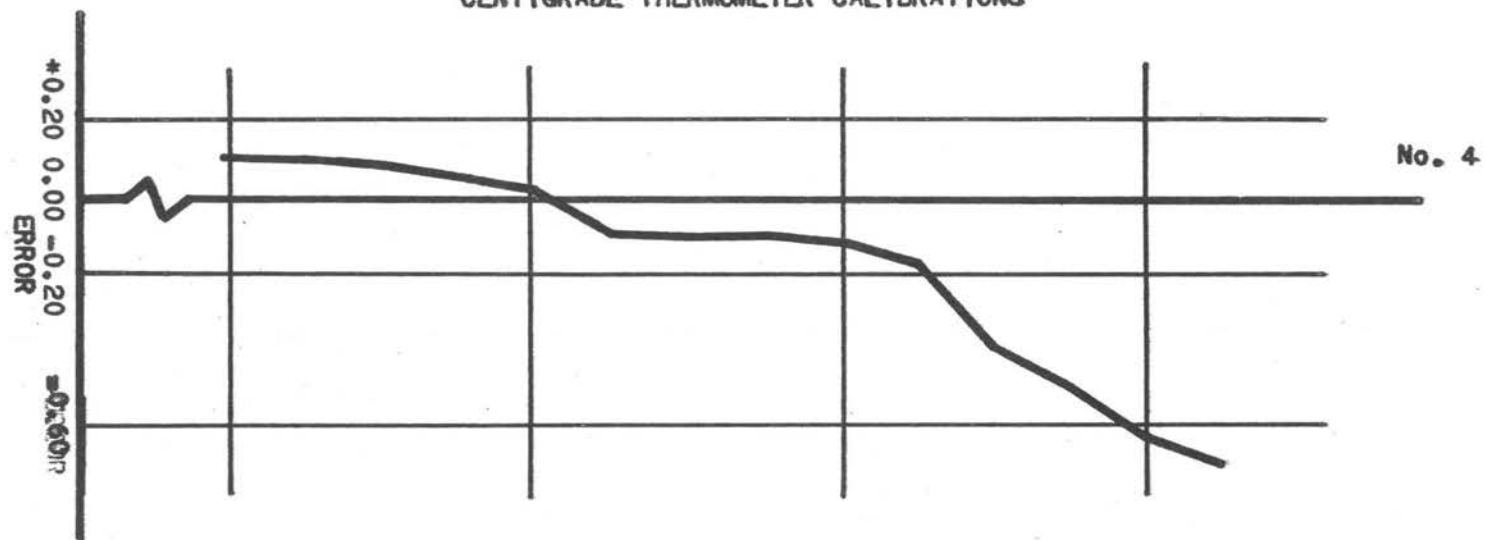


FIGURE 24  
FAHRENHEIT THERMOMETER CALIBRATIONS

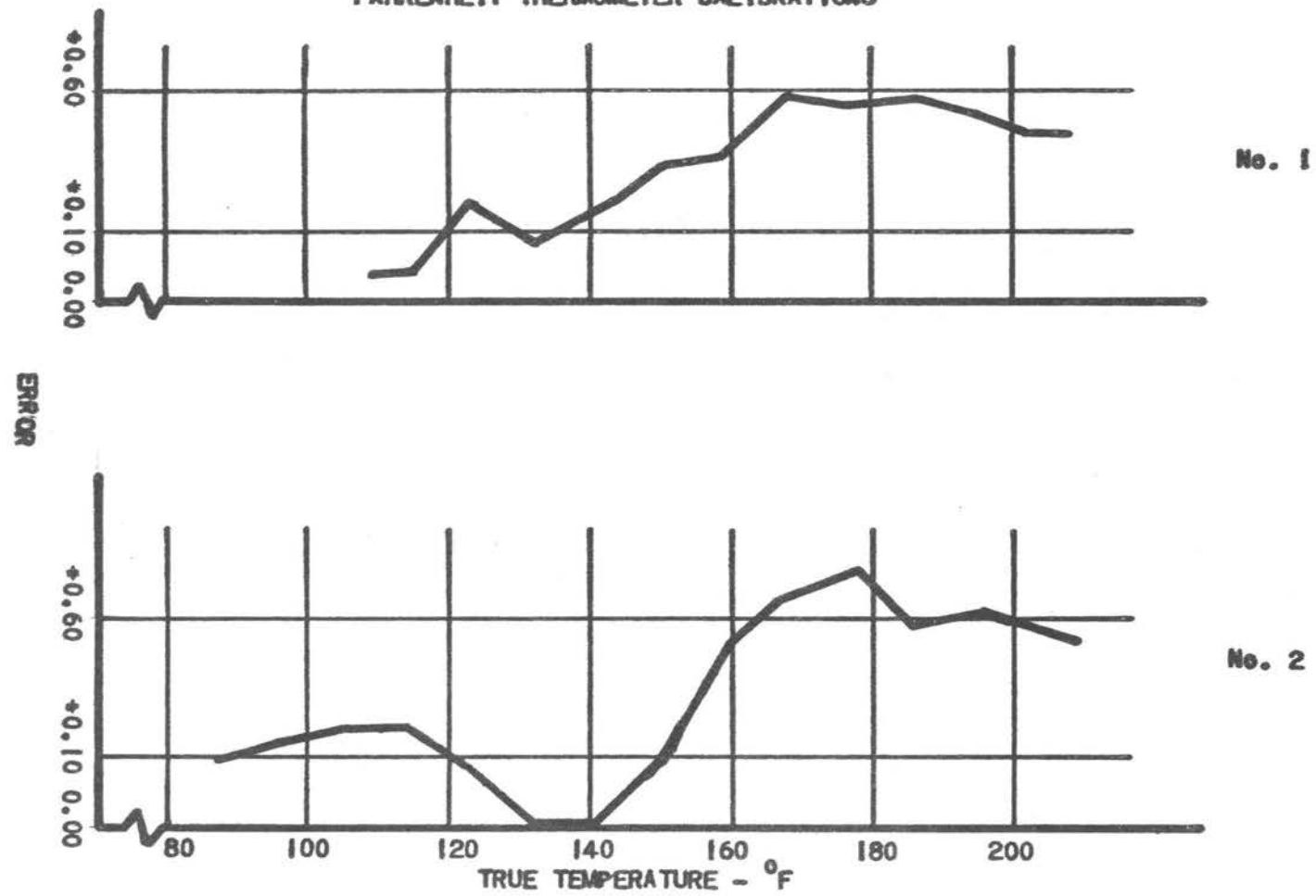


FIGURE 25  
FAHRENHEIT THERMOMETER CALIBRATIONS

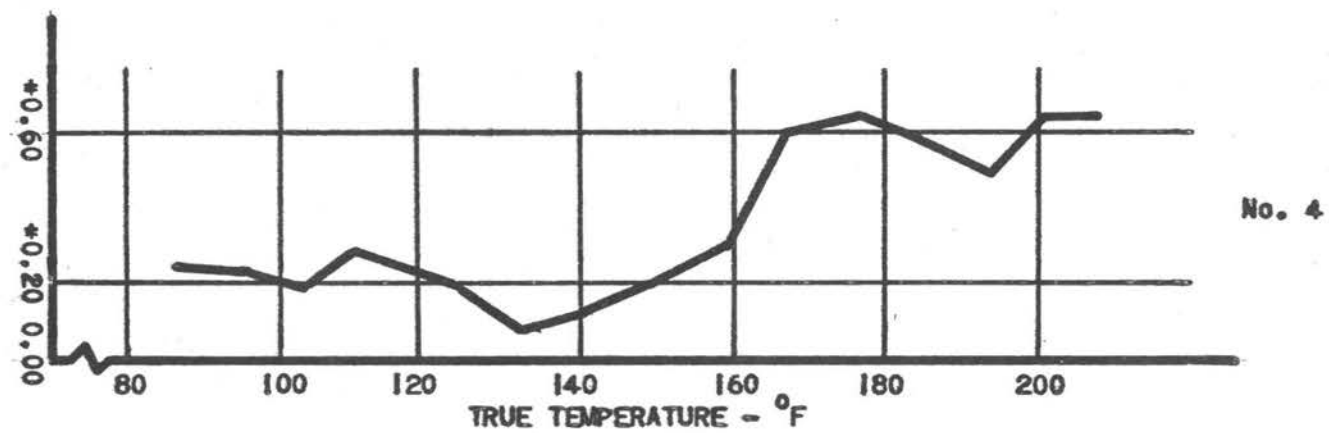
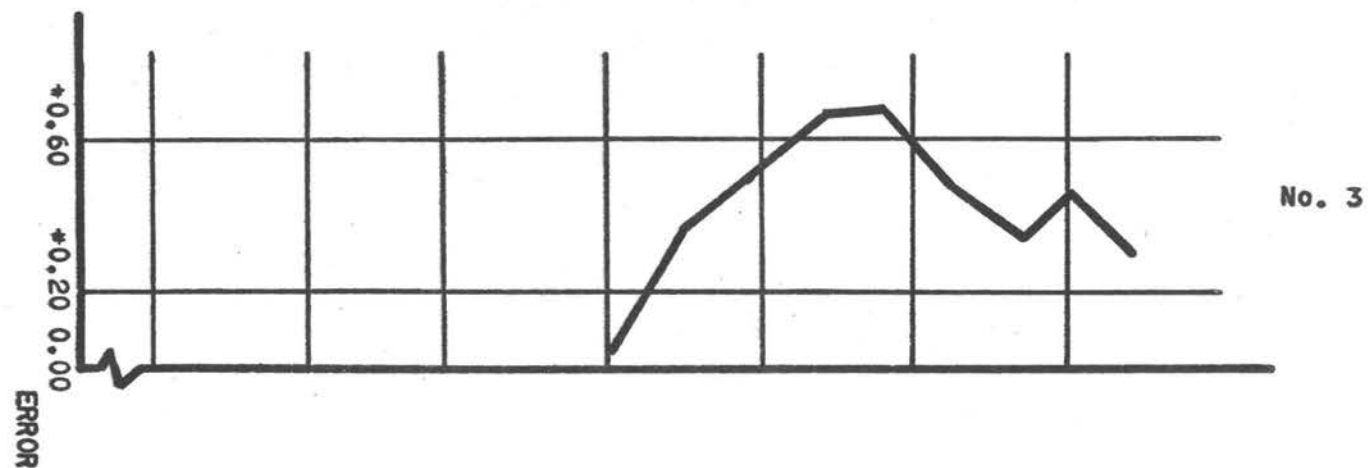


FIGURE 26  
COLD STREAM MANOMETER CALIBRATION

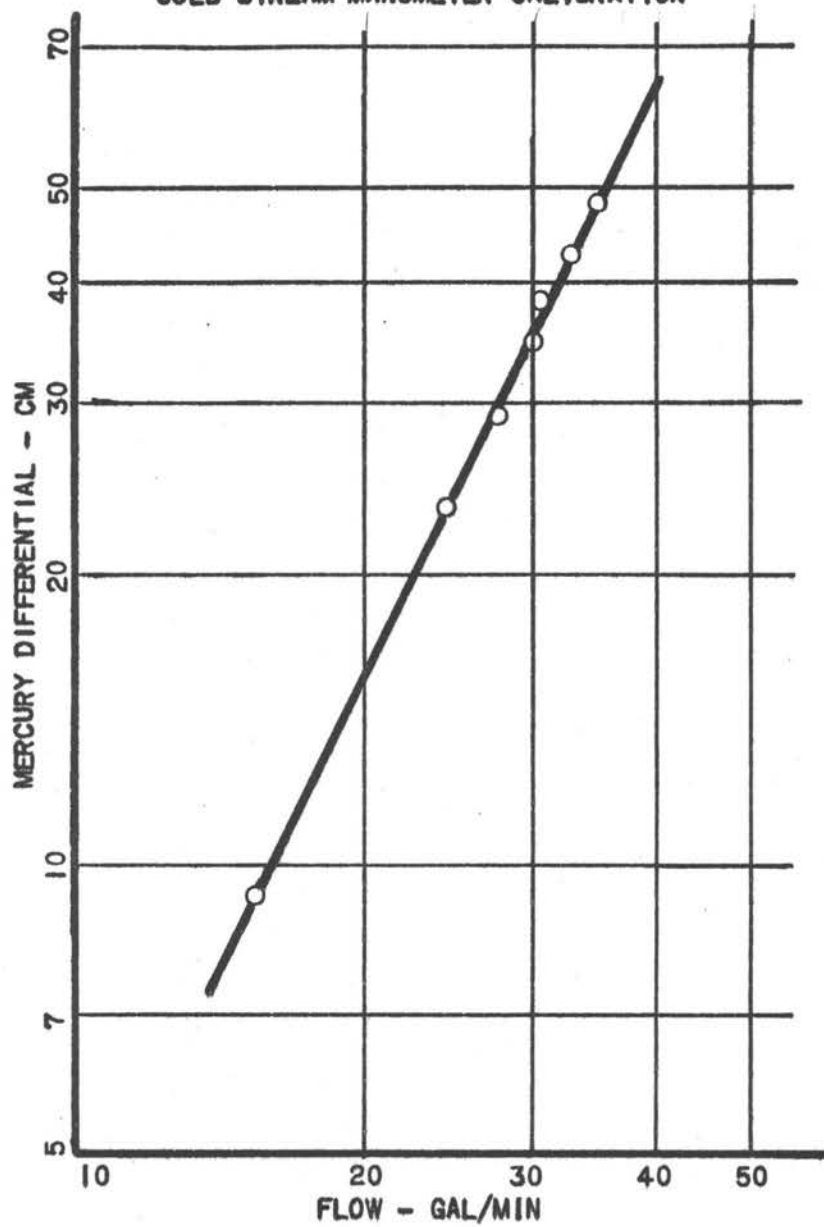
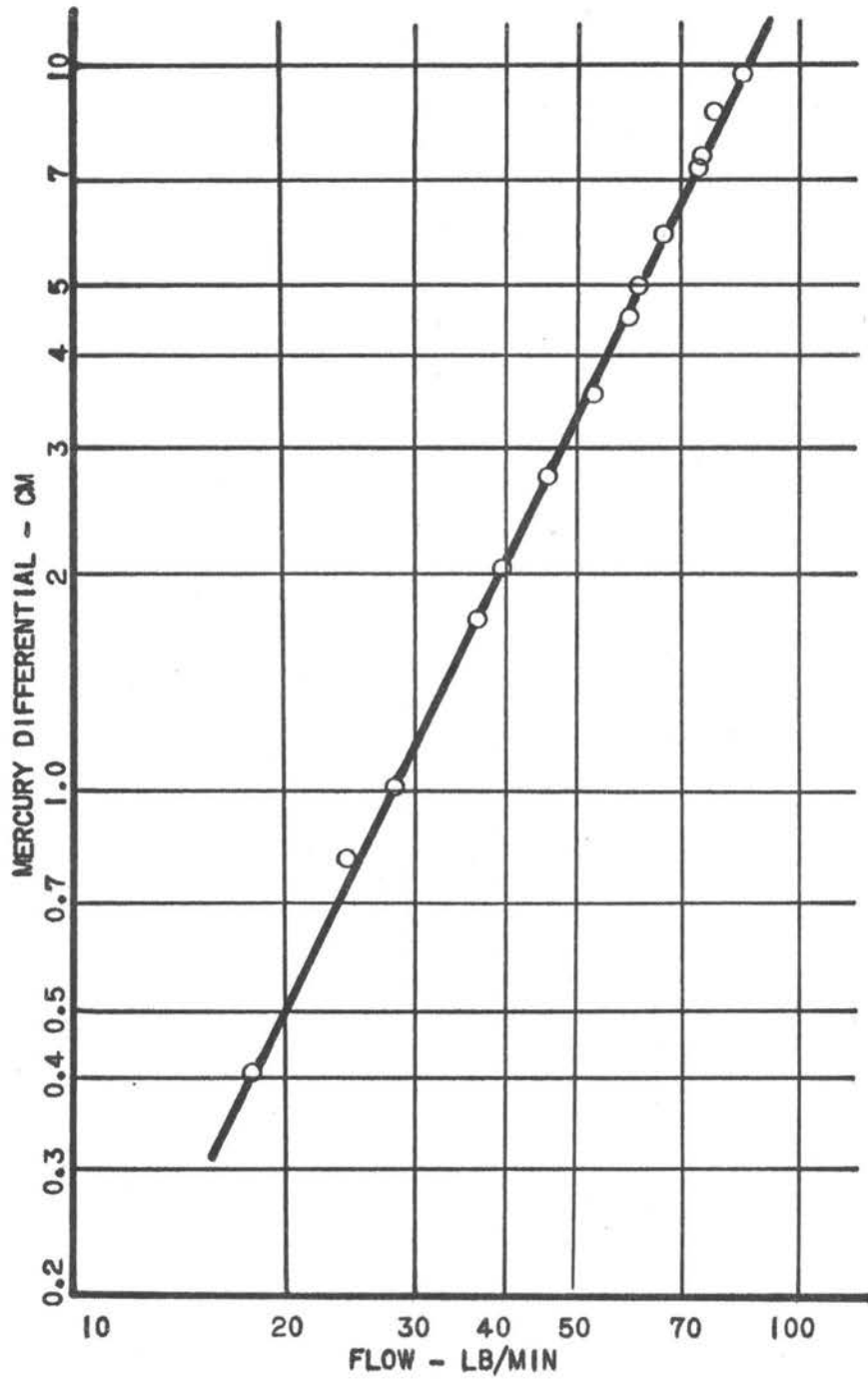




FIGURE 27

HOT STREAM MANOMETER CALIBRATION



## SAMPLE CALCULATIONS

1 - Calculation of a point for a Wilson plot.

Example: A point for the 9 fin/inch tube Wilson plot.

	Cold Stream	Hot Stream
inlet temperature*	39.61°C	76.00°C
outlet temperature*	42.31°C	48.17°C
temperature difference	2.70°C = 4.86°F	27.83°C = 50.09°F
Flow rate manometer differential head	46.8 cmHg = 34.0 GPM (Fig. 26)	1.0 cmHg = 28.1 lb/min (Fig. 27)

\*Corrected for calibration (Figures 22, 23, 24, and 25).

Calculation of heat balances:

Cold stream -

$$(34.0 \text{ Gal/min})(60 \text{ min/hr})(\text{cuft}/7.481 \text{ Gal})(62.4 \text{ lb/cuft}) \\ (1.0 \text{ BTU/hr } ^\circ\text{F})(4.86^\circ\text{F}) = 81,920 \text{ BTU/hr.}$$

Hot stream -

$$(28.1 \text{ lb/min})(60 \text{ min/hr})(1.0007 \text{ BTU/hr } ^\circ\text{F})(50.09^\circ\text{F}) = \\ 84,510 \text{ BTU/hr.}$$

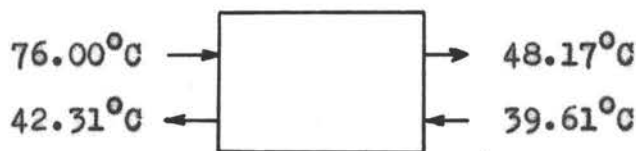
Average heat transfer rate -

$$(1/2)(81,920 + 84,510) = 83,220 \text{ BTU/hr.}$$

Determination of the heat transfer area:

The outside area on the 9 fin/inch tube is 6.496 sqft.  
(Table I)

Calculation of the log - mean temperature difference:



$$\Delta t_1 = \frac{33.69^{\circ}\text{C}}{60.64^{\circ}\text{F}} =$$

$$\Delta t_2 = \frac{8.56^{\circ}\text{C}}{15.41^{\circ}\text{F}} =$$

Corrected for calibration (Figures 22, 23, 24, and 25)

$$\Delta t_{lm} = \frac{\Delta t_1 - \Delta t_2}{\ln \frac{\Delta t_1}{\Delta t_2}} = \frac{60.64 - 15.41}{\ln \left( \frac{60.64}{15.41} \right)} = 33.01^{\circ}\text{F}.$$

Calculation of the overall coefficient,  $U_o$ :

$$U_o = \frac{(83,220 \text{ BTU/hr})}{(6.496 \text{ sqft})(33.01^{\circ}\text{F})} = 388.0 \text{ BTU/hr-sqft-}^{\circ}\text{F}.$$

$$1/U_o = 0.002577 \text{ hr-sqft-}^{\circ}\text{F/BTU}.$$

Calculation of the annular fluid velocity:

The effective flow area of the annulus is (Figure 3):

$$\frac{\pi (D_2)^2}{4} - \frac{\pi (D_f)^2}{4} = \frac{\pi}{(4)(144)} \left[ (1.506)^2 - (0.874)^2 \right] =$$

$$0.008204 \text{ sqft}.$$

The cold stream flow manometer differential head is  
46.8 cmHg = 34.0 Gal/min. (Figure 26)

$$V = \frac{(34.0 \text{ Gal/min})(\text{min}/60 \text{ sec})(\text{cuft}/7.481 \text{ Gal})}{(1/0.008204 \text{ sqft})} = 9.234 \text{ ft/sec}.$$

$$1/(V)^{0.87} = 0.1466$$

The calculation of a point on a Wilson plot is now complete since a point on the plot is fixed by  $1/U_0$  and  $1/(V)^{0.87}$ .

2 - Calculation of a point for a scaling plot.

$U_0$  is calculated exactly the same as in the Wilson plot sample calculation. The time interval is calculated from the difference between the day and time of the first reading (one hour after start up) and the day and time of the reading being calculated. This is a complete calculation of a point on a scaling plot since a point on the plot is fixed by  $U_0$  and the elapsed time.